國立交通大學

生物科技研究所

碩士論文

創傷弧菌 YJ016 中一段與致病相關基因群組的功能探討

Analysis of a virulence-associated genomic island in *Vibrio vulnificus* YJ016

研究生：楊祐俊

學號：9228510

指導教授：彭慧玲博士

中華民國　94 年 7 月

中文摘要

在創傷弧菌 YJ016 的小染色體上，我們找到了一個與致病相關的基因群組 (VVA0325 至 VVA0334)，其中有一個 RtxL 被歸類為“多重覆片段毒素” 家族中一個成員，以及一套第一型的運送系統，和包含一個感應子與四個調控子的訊息傳遞系統。為了要分析 rtxL 以及包含一個 GGDEF 功能區域的 VVA0326 和一個包含 EAL 功能區域的 VVA0328，利用同源互換的原理，我們分別建構了這三個特定基因缺損的突變株。與霍亂弧菌中的細胞毒素 RtxA 一樣，RtxL 也是一個巨大的蛋白質，在長達 4655 個胺基酸序列中，我們發現了三個長 539 的重覆片段，然而，在細胞毒殺能力的實驗中卻發現，*rtxL* 缺損株的毒殺能力比較野生株並沒有明顯的差異，也就是說 RtxL 並不像 RTX 家族中的其它成員一樣扮演細胞毒素的角色。缺損了包含一個 GGDEF 功能區域的突變株 VVA0326$^-$，培養在 LB 的洋菜膠上，呈現出較小的生長菌落，在測定單位菌落數的結果發現，VVA0326$^-$在生長速度上，相較於野生株並沒有不同，因此我們推論生長速率並不是造成菌落變小的主要因子，除此之外，VVA0326$^-$在游泳的分析培養皿中游的比野生株快，在 CAS 的分析培養皿上，與野生株比較，VVA0326$^-$有比較好的生長狀態，而缺損了包含一個 EAL 功能區域的突變株 VVA0328$^-$，卻有被抑制生長的現象，可能是因為突變株影響了表面的結構，進而改變了細菌對於 HDTMA 的敏感層度。此外，我們也發現這兩個蛋白質會有聚集在細菌兩端的行為。

根據 pfam 資料庫 (Version 17.0)，我們整理同時擁有 GGDEF 和 EAL 功能性區域的蛋白質 (GGDEF-EAL)，這些蛋白質可以被區分成兩種型態，在總數 621 個 GGDEF-EAL 中有高達 606 個是 A 型態，而且它在古老的細菌 *Aquifex aeolicus* VF5 的基因體中也能找到，因此我們推測它可能是 GGDEF-EAL 的祖先，藉由分析創傷弧菌中所包含之 GGDEF 和 EAL 的演化關係，大部份的 GGDEF-EAL 會群聚在樹型相近的位置，進一步比較在 EAL 樹型上有鄰近關係的蛋白質序列，根據他們的長度、與所包含的功能區域，我們找到了一些重製的演化痕跡，這樣的結果指出，目前看到大多數的 GGDEF 和 EAL 可能都是經過重製產生。

Abstract

A virulence-associated genomic island (VVA0325 to VVA0334) was annotated on the small chromosome of *Vibrio vulnificus* YJ016, which contains a gene cluster encoding a large protein RtxL of RTX (repeat in toxin) family, a type I secretion system, and a signal transduction system composed of a sensor and four regulators. In order to analyze the functional roles of *rtxL,* and VVA0326 and VVA0328, encoding respectively GGDEF- and EAL- proteins of signal transduction system, the gene specific deletion mutants were constructed by gene replacement via homologous recombination. Similar to the large size of *V. cholera* cytotoxin RtxA, RtxL encodes a protein of 4655 aa containing three repetitive peptides of 539 aa. However, no obvious difference was observed between wild-type and the *rtxL*$^-$ mutant in cytotoxicity assay suggesting that RtxL is not a cytotoxin as the other members of RTX family. The VVA0326$^-$ mutant carrying a deletion of the GGDEF domain displayed smaller colony morphology on LB plate while compared to the wild type. No difference in colony forming units was found indicating that growth rate is not likely a major factor to confer the phenotype of small colony. In addition, VVA0326$^-$ appeared to swim better than wild type bacteria on the swimming plate. VVA0326$^-$ grew better, while VVA0328$^-$ mutant, which carried a deletion of the EAL domain, grew worse than wild type when the bacteria were cultured on CAS plate at 30°C. This implied that changes in surface structures of the mutants affected the bacterial susceptibilities to HDTMA contained in CAS plate. Furthermore, subcellular localization analysis revealed that the two GGDEF- and EAL- proteins tended to localize at the cell poles.

According to the domain organization, the GGDEF-EAL containing proteins (pfam database, version 17.0) were classified into A and B types. Six hundreds and

five of the 621 proteins were in A type, which was also found in the ancient bacteria *Aquifex aeolicus* VF5 suggesting that this is the ancestor of the GGDEF-EAL proteins. Phylogenetic analysis of GGDEF- and EAL- containing proteins in the genome of *V. vulnificus* YJ016 revealed that GGDEF-EAL proteins were clustered. Comparative analysis of domain organization of the clads in the EAL tree allowed identification of several duplication events. The results indicated that most of the GGDEF- and EAL-containing proteins arised by gene duplication.

致謝

回想兩年來的碩士生涯，一種感恩的心情油然而生，在此謝謝陪著我一塊成長的大家，感謝各位不論是在學術上或是日常生活中所提供的協助，支持我走過人生中重要的學習過程。

這本論文能夠順利的完成，最要感謝的是我的指導教授 彭慧玲老師，除了在實驗上的指導與鼓勵，老師在生活上也提供了我很多寶貴的意見，尤其這本論文讓您花了很多心思，在此致上最深切的感激。更要感謝口試委員 黃秀珍與 楊昀良老師在口試期間所提供的細心指證與建議，才能使得本篇論文更趨於完善。除此之外，謝謝怡琪學姐在實驗技術與經驗的分享，讓我能夠順利的完成碩士論文。

對於實驗室的同仁，我們一塊經歷過好多美麗的回憶，謝謝漂亮的阿婷與可愛的小九，不論是在研究或者是生活上的鼓勵，六年的感情不是簡單的幾句話就能道盡，祝福妳們都能找到幸福。至於我的同學小誠與小新，我的小花小草就交給你們照顧了，有空一定要記得要來我”討論學術“喔！另外還要謝謝曾經一塊打拼的學長姐：榕華、怡欣、騰逸、巧韻、致翔、定宇、美甄、婉君、珮瑄、平輝，以及熱心的育聖、細心的智凱、美麗的心瑋，因為有大家的幫忙，讓我在求學的過程中增添了很多溫暖與歡笑，謝謝你們。

最後感謝爸爸、媽媽、三姐對我的照顧，以及最重要的怡伶，你們是我精神上最大的支持，僅以此論文獻給我的家人以及關心我的人。

Contents

Lists of the tables and figures

Abbreviation:

AP	Alkaline phosphatase
BCIP	5-bromo-4-chloro-3-indolyl phosphate
BLAST	basic local alignment search tool
bp	base pair(s)
bvg	*Bordetella* virulence gene
CFU	colony forming unit
CPS	capsular polysaccharide
DIG	digoxigenin
DTT	dithiothreitol
EDTA	ethylenediamine-tetraacetic acid
HMM	hidden Markov model
IPTG	isopropyl-β-D-thiogalactopyranoside
kD	kiloDalton(s)
LB	Luria-Bertani medium
NBT	Nitro blue tetrazolium
PBS	Phosphate-buffered saline
PCR	Polymerase Chain Reaction
rpm	revolutions per minute
RTX	repeats in toxin
SDS	sodium dodecyl sulfate
SDS-PAGE	SDS polyacrylamide Gel Electrophoresis
TEMED	N, N, N, 'N'-Tetramethylethylenediamine
Tris	Tris(hydroxymethyl)-aminomethane

Introduction

1. Clinical importance of *Vibrio vulnificus*

Vibrio vulnificus, a motile Gram-negative curved rod-shaped bacterium with a single polar flagellum is an opportunistic pathogen causing rare and yet devastating disease (Strom and Paranjpye, 2000). It commonly exists in marine environment and is a naturally occurring, free-living inhabitant of estuarine throughout the world. Infection by *V.vulnificus* occurs through the consumption of raw oysters or contamination of wounds and causes complications including an invasive septicemia and wound infections (Hoi *et al.*, 1998). It has been shown as the leading cause of reported death from seafood in the United States, which is approximately 40 cases per year (Hlady *et al.*, 1993; Hlady and Klontz, 1996). In Taiwan, between 1996 and 2000, the number of *V. vulnificus* infection ranged from 13 to 26 cases per year (Hsueh *et al.*, 2004). These diseases share the characteristics of extensive damage caused by extremely rapid multiplication of the bacteria in host tissue.

Despite the virulence analysis using a combination of animal and cell culture models for over 20 years, surprisingly little is known about the pathogenic mechanisms of *V. vulnificus*. Up to now, some factors including an extracellular hemolysin/cytolysin (Gray and Kreger, 1989), an elastolytic protease (Oliver *et al.*, 1986), the capability of iron acquisition (Biosca *et al.*, 1996), a polysaccharide capsule (Wright *et al.*, 1993) and an endotoxic lipopolysaccharide (McPherson *et al.*, 1991), and serum resistance activity (Johnson *et al.*, 1984) have been implicated as possible virulence determinants for *V. vulnificus*.

2. A virulence-associated genomic island

Vibrios, which are gram-negative halophilic bacteria that include more than 60 species, comprise the major culturable bacteria in marine and estuarine environments. They commonly possess two chromosomes and that the genome structure consisting of a maintained relatively flexible and smaller chromosome and a large chromosome retaining most of the essential genes is stably among species of the family *Vibrionaceae* (Okada *et al.*, 2005)

The sequenced genome of *V. vulnificus* YJ016 also includes two chromosomes of estimated 3377 kbp (large chromosome) and 1857 kbp (small chromosome) in size, and a plasmid of 48,508 bp. Five groups of putative pathogenicity genes encoding respectively the proteins for type IV pilus, capsular polysaccharide biosynthesis, iron acquisition, extracellular enzyme and toxin, and RTX [repeats in toxin] toxin were annotated (Chen *et al.*, 2003).

The sequence analysis revealed an RtxA gene cluster (VVA1030, VVA1032, VVA1034, VVA1035 and VVA1036) contained in a 22-k bp region on the small chromosome. Interestingly, an additional RTX like gene (RtxL), VVA0331, was annotated also on the small chromosome. A typical type I secretion system encoding gene cluster (VVA0332-VVA0334) and a signal transduction system encoding gene cluster (VVA0325-VVA0329) containing an originally named VieSAB like three component system were found to be located respectively upstream and downstream flanking the RtxL gene (Fig. 1A). We speculate that the three gene clusters function coordinately as a virulence-associated genomic island and roles of the genomic island in the bacterial virulence were hence investigated.

2-1. RTX toxins

RTX toxins play an important role in the virulence of a variety of human and animal gram-negative bacterial pathogens. There are two categories: the hemolysins, which affect a variety of cell types, and the leukotoxins, which are cell-type and species-specific (Lally *et al.*, 1999). It is one of a close family of membrane-targeted toxins, which have been shown to be influential not only in urinary tract infections but also hemorrhagic intestinal disease, juvenile periodontitis, pneumonia, whooping cough, and wound infections; these toxins include enterohemorrhagic O157 *E. coli* hemolysin (Schmidt *et al.*, 1996), the leukotoxin of *Pasteurella haemolytica* (Strathdee and Lo, 1987), the hemolysins and leukotoxins of *Actinobacillus* spp (Burrows and Lo, 1992; Frey *et al.*, 1993; Kraig *et al.*, 1990), the bifunctional adenylate cyclase-hemolysin of *Bordetella pertussis* (Glaser *et al.*, 1988), and the hemolysins of *Proteus vulgaris* (Welch, 1987), *Morganella morganii* (Koronakis *et al.*, 1987), and *Moraxella bovis* (Gray *et al.*, 1995).

They commonly share a posttranslational maturation and a C-terminal calcium-binding domain of acidic glycine-rich nonapeptide repeats that has led to the RTX family nomenclature. In addition, they are exported out of the cell by type I secretion system (Welch, 2001). The posttranslational modification is unique to this toxin family, but Ca^{2+} binding and type I secretion are both common to other bacterial proteins (Stanley *et al.*, 1998; Welch, 2001). In *E. coli* HlyA, there are 11 to 17 glycine-rich repeats. When the protein bound with Ca^{2+} (one calcium ion per repeat), it forms short β-strands organized in an unusual "spring-like" structure called a parallel β-barrel or β-superhelix (Baumann *et al.*, 1993). Calcium binding is an absolute requirement for its cytotoxic activity (Boehm *et al.*, 1990; Ludwig *et al.*, 1988) and the binding occurs following its export action.

2-1-1.VcRtxA

In *V. cholerae*, RtxA encoding gene was identified as a 13,635-bp-long ORF located adjacent to *ctx* (cholera toxin) genes on the large chromosome (Lin *et al.*, 1999). The deduced *V. Cholerae* RtxA (VcRtxA) protein with 4,545 aa in length is the second largest single-polypeptide toxin known, which caused cell rounding and depolymerization of the actin cytoskeleton in a broad range of cell types (Boardman and Satchell, 2004; Fullner and Mekalanos, 2000; Lin *et al.*, 1999). Like other RTX toxins, VcRtxA shares the common features of posttranslational maturation depending on RtxC activator, a C-terminal calcium-binding domain of acidic glycine-rich nonapeptide repeats, and their exportation out of the cell by type I secretion system, RtxB and RtxD (Boardman and Satchell, 2004; Lin *et al.*, 1999; Sheahan *et al.*, 2004; Welch, 2001).

2-1-2.VvRtxA

In *V. vulnificus* YJ016, VvRtxA protein with 5206 aa in length is the largest single-polypeptide toxin known. Comparison of the amino acid sequences of VcRtxA and VvRtxA revealed 80–90% identity throughout most regions of the toxins. VvRtxA also exerts the common features of all RTX toxins, including the GD-rich calcium binding repeats at the C-terminus and N-terminal hydrophobic repeats. Although RtxL was annotated as a second RTX protein and an entire type I secretion gene cluster is also present downstream of the RtxL encoding gene, no typical feature of RTX toxin could be identified in the 4655 aa sequences yet.

2-2. Signal transduction- two component systems (2CSs)

To subsist in nature, bacteria possess regulatory systems that permit them to recognize and adapt to a highly changing environment. The capacities are brought about largely through varying in gene expressions that are coordinated by global

regulatory networks. Pathogenic bacteria often use two-component systems (2CSs) to control expression of the genes encoding bacterial toxins, adhesions, and other virulence-associated molecules that promote their survival in the host (Locht, 1999).

Bacterial 2CS consisting of a sensor histidine kinase and a response regulator, acts to recognize specific signals and to convert this information into transcriptional or behavioral responses in order to confront the highly changing circumstances (Miller *et al.*, 1989; Soncini and Groisman, 1996; Stock *et al.*, 1989). After sensing the input signals, the sensor protein catalyzes an autophosphorylation reaction, which transfers a phosphate from ATP to a conserved histidine residue. The phosphate group is subsequently transferred from the histidine residue to a specific aspartate residue on the receiver domain of the cognate response regulator. Phosphorylation of the response regulator leads to activation of the transcription-regulating activity through an appropriate conformational change (Mizuno, 1998; West and Stock, 2001).

2-2-1. VieSAB three component system

VieSAB of *V. cholerae* differs from the conventional 2CS in that two putative response regulators, VieA and VieB, are contained in the system and hence named three component system. Different from VieB which has a typical N-terminal phosphoreceiver domain of response regulator but lacking any recognizable DNA binding motif, the *vieA* gene encodes a response regulator with a LuxR-family type of DNA binding motif and an EAL domain (Galperin *et al.*, 2001). Evidences from two different *in vivo* screenings have suggested that VieSAB contributes to regulate the gene expressions during infection, such as CT (cholera toxin) production (Camilli and Mekalanos, 1995; Lee *et al.*, 2001; Tischler *et al.*, 2002). The *vieSAB* genes adjacent to each other appeared to be transcribed differentially. Although both *vieS* and *vieA* expressed during in vitro growth, the expression of *vieS* appeared to be constitutive, while *vieA* expression was VieA dependent (Lee *et al.*, 1998). VieA has been shown to control the intracellular concentration of cyclic diguanylate (cyclic di-GMP) through its EAL domain carrying a cyclic di-GMP phosphodiesterase activity. The

level of cyclic di-GMP, which is likely a secondary messenger in the cells, led to an optimal expression of *vps* (*Vibrio* exopolysaccharide synthesis) (Tischler and Camilli, 2004)

2-3. Cyclic diguanylate as a secondary messenger

In addition to 2CS, bacteria also use receptor mediated signaling system, so-called secondary messenger as a linker between extracellular signals and the downstream events (Galperin, 2004). Cyclic nucleotides (cAMP and cGMP) are among the most widely studied of this class of molecules (Botsford, 1981; Botsford and Harman, 1992). Recently, a new signaling molecule, cyclic-di(3'→5')-guanylic acid (cyclic di-GMP), was identified as an allosteric activator in cellulose biosynthesis pathway in *Gluconacetobacter xylinus* (Ross *et al.*, 1990). In addition, the involvement of the GGDEF- and EAL- containing proteins in cyclic di-GMP metabolism has been established, whereby the GGDEF domain represents the dinucleotide cyclase, while EAL, most probably, represents the cyclic dinucleotide phosphodiesterase (Ausmees *et al.*, 2001; Simm *et al.*, 2004; Tal *et al.*, 1998).

2-3-1. Biological function of GGDEF- and EAL- containing proteins

The GGDEF domain dubbed based on its conserved sequence motif (170 aa defined in HMM profile) was firstly discovered in the response regulator PleD that controls cell differentiation in the swarmer-to-stalked cell transition in *Caulobacter crescentus* (Hecht and Newton, 1995) and the EAL domain dubbed based on its conserved sequence motif (245 aa defined in HMM profile) was originally described in a study of virulence related to the 2CS BvgR in *Bordetella pertussis* (Merkel et al., 1998). Up to now, the mass sequencing of bacterial genomes detected an abundance of GGDEF and EAL containing proteins (Galperin *et al.*, 2001). In the sequenced prokaryotic genomes, 1601 and 1016 copies of GGDEF and EAL domain respectively,

have been found and 147 and 88 representative architectures of GGDEF and EAL domain were defined according to Pfam database (http://www.sanger.ac.uk/Software/Pfam/). More and more experimental data of GGDEF and EAL proteins have been reported with time, and the biological functions of them were marshaled as below:

Aggregative behavior and biofilm formation

Several experimental evidences have shown that GGDEF and EAL containing proteins influence the bacterial morphotypes, which have been characterized by an increased production of extracellular matrix components, such as fimbriae and exopolysaccharide, by aggregative behavior and by enhanced biofilm formation. Some GGDEF or EAL protein homologs have been identified as regulators of this adhesive behavior. In *Salmonella*, AdrA, a GGDEF protein, is required for cellulose synthesis but not for the formation of aggregative fimbriae (Romling *et al.*, 2000; Zogaj *et al.*, 2001). In *Pseudomonas*, WspR, a CheY-GGDEF protein, controls the expression of an acetylated cellulose polymer and a fimbrial component of the biofilm matrix (Spiers *et al.*, 2002; Spiers *et al.*, 2003) and PvrR, a CheY-EAL protein, has been described as a regulator of biofilm formation and aggregation (Drenkard and Ausubel, 2002). Besides, RocS and MbaA, GGDEF-EAL proteins, were both identified in genetic screens for *V. cholerae* mutants defective in biofilm formation and maturation. The *rocS* mutant seemed to possess a general defect in switching to the rugose phenotype (Rashid *et al.*, 2003). MbaA was shown to be also required at a later stage of biofilm formation (Bomchil *et al.*, 2003).

Bacterial motility

There are experiments suggesting that cyclic di-GMP acts as a messenger to direct the transition from sessility to motility (Simm *et al.*, 2004) and some GGDEF-EAL protein homologs have been identified. In *V. parahaemolyticus*, SrcC

controls swarmer cell differentiation, including the production of lateral flagella and synthesis of capsular polysaccharide in order to grow on surfaces (Boles and McCarter, 2002; Guvener and McCarter, 2003). MorA is a regulator of GGDEF-EAL protein affecting flagellar development and biofilm formation in diverse *Pseudomonas* species (Choy *et al.*, 2004). FimX, another GGDEF-EAL protein, is required for the bacterial type IV pilus-mediated twitching motility (Huang *et al.*, 2003). Additionally, in *Caulobacter crescentus*, cells that lack functional PleD, a CheY-GGDEF protein, are hypermotile, unable to eject the flagellum during the swarmer-to-stalked cell transition, and failing to fully synthesize a stalk structure (Aldridge and Jenal, 1999; Aldridge *et al.*, 2003).

3. Specific aims

In this study, we aimed to investigate the likely roles of the GGDEF-containing protein VVA0326, the EAL-containing protein VVA0328 and RtxL. The specific experiments performed are as following:

1.1. Several *Vibrio vulnificus* YJ016 derived mutants carrying respectively VVA0326, VVA0328 and RtxL gene deletion were constructed. Phenotypic analysis of the mutants including growth rate analysis, biofilm formation assay, swimming motility, flagellar and exopolysaccharide synthesis were carried out.

1.2. VVA0326-GFP and VVA0328-GFP (Green Florescence Protein) fusion protein constructs were obtained to demonstrate the localized distribution of the overexpressed proteins in *E. coli* JM109.

2. We have also employed phylogeny analysis to study the evolutionary relationship of GGDEF- and EAL- containing proteins in the bacteria.

Materials and methods

1. Plasmids, bacterial strains, and growth conditions

The bacterial strains and plasmids used in this study are listed in Table 1 and 2. The bacteria were propagated at 37 °C in Luria-Bertani (LB) broth or the medium supplemented with appropriate antibiotics which include kanamycin (25 μg/ml), ampicillin (100 μg/ml), polymyxin B (100 U/ml). The density of the bacterial culture was determined by measuring the optical density at 600 nm (OD_{600}).

2. Bioinformatics analysis

Homology search analysis and gene annotation were performed with BLAST analysis in NCBI (http://www.ncbi.nlm.nih.gov) and HMM-profile search in Pfam database (http://www.sanger.ac.uk/Software/Pfam/). Signal peptide identification and the prediction of transmembrane regions were carried out respectively by SignalP 3.0 (Bendtsen *et al.*, 2004), LipoP 1.0 (Juncker *et al.*, 2003) and TopPred 2 (von Heijne, 1992).

3. Recombinant DNA technique

The recombinant DNA experiment was carried out by standard procedures as described (Sambrook and Russell, 2001). Plasmid DNA was prepared by VIOGENE Miniprep kit (Gene-Spin^{TM}-V^2). Restriction endonucleases and DNA modifying enzymes were purchased from MBI (Fermentas, Hanover, MD), and were used according to the recommendation of the suppliers.

4. Construction of VVA0326, VVA0328 and VVA0331 deletion mutants

The individual deletions in VVA0326, VVA0328 and VVA0331 were introduced into chromosome of *V. vulnificus* YJ016 by allelic exchange strategy. The primer sets used for PCR amplification are listed in Table 3. As shown in Fig.1, approximately 1000-bp sequences flanking both sides of the deleted region were cloned into plasmid pCVD442 (Donnenberg and Kaper, 1991), a suicide vector containing *SacB* gene which allowed a positive selection with sucrose for loss of the vector, to generate an in frame deletion plasmid, pVV3-4, pVV7-8 and pVV9-10. The resulting plasmids were then mobilized to *V. vulnificus* YJ016 through conjugation from *E. coli* S17-1 λ *pir*. The transconjugants, which had pVV3-4, pVV7-8 and pVV9-10 integrated in the chromosome via homologous recombination, were selected by ampicillin (100 mg/ml) and ploymyxin B (100U/ml), and tested for sensitivity to 10% sucrose. One of the "sucrose-sensitive" transconjugants was subsequently grown in LB containing 10% sucrose at 37 °C overnight and then the culture spread onto a 10% sucrose-containing plate for selection the "sucrose-resistant" clones. The resultant strains were further tested for ampicillin sensitivity, and confirmed using PCR and Southern blot hybridization. The resulting bacteria with mutation in each of VVA0326, VVA0328 and VVA0331 were named respectively VVA0326$^-$, VVA0328$^-$ and RtxL$^-$.

5. Southern blot analysis

Chromosomal DNA was prepared from overnight cultures of either *V. vulnificus* YJ016 or the derived bacteria grown in LB medium. After digesting the DNA with restriction endonucleases, the DNA fragments were resolved on 1% agarose gels by electrophoresis and transferred to nylon membrane (Amersham Pharmacia Inc.).

Finally, the membranes were hybridized with either of the probes to confirm the mutation of each of the VVA0326$^-$, VVA0328$^-$, VVA0326$^-$VVA0328$^-$ and RtxL$^-$ strains.

6. Cytotoxicity assay

The cytotoxicity of *V. vulnificus* strains was determined with HEp-2 cells, a human laryngeal carcinoma cell line. The cells were maintained in Earle's minimal essential medium (MEM) containing 10% fetal calf serum and 40 mg of gentamicin per ml. Cytotoxicity was assayed after treatment of cells with bacterial suspension. HEp-2 cell suspension (0.2 ml) was plated at a density of 3 x10^5/ml in each well of a 24-well tissue culture plate coated with 0.1% bovine serum albumin, and the cells were grown at 37°C to confluence. The cell monolayer was washed and then added with 180 ml of Earle's MEM. In the experiment, the monolayer was infected with washed bacteria (suspended in PBS) at a multiplicity of infection (MOI) of 10. After incubation at 37°C for either 2 h or 4 h, the cytotoxicity was determined by measuring the activity of lactate dehydrogenase (LDH), a cytosolic enzyme released upon cell lyses, in the supernatant. LDH activity was assayed with a commercial kit (CytoTox 96 nonradioactive cytotoxicity assay; Promega) and was expressed as % Cytotoxicity = (Experimental – Effector Spontaneous – Target Spontaneous) / (Target Maximum – Target Spontaneous) ×100%

6. Swimming assay

Tryptone swimming plates were composed of 0.3% Bacto Agar, 1% NaCl, and 1% tryptone. Bacteria were inoculated with a sterile tip and incubated for 6 and 9 h at

37 °C and 30 °C (Kohler *et al.*, 2000).

7. Quantitation of biofilm formation

Biofilm formation was assessed by the ability of the cells to adhere to the walls of 96-well microtitre dishes made of PVC (TPP 96 flat) with some modification of the reported protocol (O'Toole and Kolter, 1998). Essentially, the indicator medium (100 μl/well) contained an aliquot of 1:10 diluted overnight bacteria culture and the plate was incubated at 30°C with shaking (150 rpm) 48 h for biofilm formation. The unadherent bacteria were washed triply with 200 μl PBS and then 200 μl of 1% crystal violet (CV) was added to each well. After the plate was placed at room temperature for 15 min, PBS was utilized to wash the plate for three times again. Finally, the CV-stained biofilm was solubilized in 200 μl of 95% enthanol and the absorbance determined at $OD_{550\,nm}$ using spectrophotometer (ELx800, BIO-TEK).

8. Purification and analysis of exopolysaccharides

Exopolysaccharides (EPSs) were purified as described previously (Whitfield and Roberts, 1999). Briefly, cells were streaked from a single colony onto the surface of LB plates and incubated for 16 h at 30°C. Cells were suspended in phosphate-saline buffer (20 mM sodium phosphate [pH 7.3], 100 mM NaCl), and culture densities were equally adjusted. The EPSs were extracted from the cell mixture with hot-phenol and phenol was removed by dialyzed against water overnight. The crude extract were then treated with DNase (4 mg/ml), RNase (0.2 mg/ml) and proteinase K (4 mg/ml) and dialyzed against water overnight again. Samples containing extracted EPSs were analyzed by sodium dodecyl sulfate-polyacrylamide gel electrophoresis (SDS-PAGE)

as described for proteins (McCarter and Silverman, 1987) with the following modifications. The gels were 8.5 cm long, with the lower (12.5% polyacrylamide) gel being approximately 2 cm and the upper (5% polyacrylamide), stacking gel being approximately 6.5 cm. The gels were made in this manner because the EPSs migrated only through the stacking gel. After electrophoresis, the gel was immediately immersed in 100 ml of Fixative solution (40% ethanol/10% acetic acid) and gently rocked for 30 min. Gel may be stored overnight at this step. The gel was then oxidized in 100 ml oxidizer solution (10% Bio-Rad oxidizer concentrate) for 5 min, and washed three times in 200 ml of dH_2O for 5 min each time. Afterward the gel was stained in 100 ml of silver Reagent (10% Bio-Rad silver concentrate) for 20 min and rinsed in dH_2O 30 sec maximum. The gel was rinsed in 100 ml of Bio-Rad developer (3.0 g/200 ml of dH2O) with agitation until dark precipitate formed and immediately drained to remove all precipitate. Finally, the color was developed with the remaining developer for 5 min. The development was stopped in 100 ml of 5% acetic acid for10 min followed by a 200 ml dH_2O.

9. Construction of VVA0326-GFP and VVA0328-GFP fusion plasmids

To examine subcellular localization of VVA0326 and VVA0328, respectively containing GGDEF and EAL domain, the coding sequences of these two genes were isolated and fused with the *gfp* fragment. As shown in Fig. 12A, the primer pairs Gp1/Gp2 and Ep1/Ep2 were used respectively to amplify the coding regions of VVA0326 and VVA0328, and also to introduce adjacent *Hin*dIII and *Kpn*I restriction sites. The PCR products were then cloned into TOPO TA Cloning vector (pCR 2.1 TOPO), which resulted of the plasmids pGGDEF and pEAL. The *Hin*dIII-*Kpn*I fragments of VVA0326 and VVA0328 were then subcloned in frame and fused to *gfp*

gene of pGFPuv (GenBank Accession #U62636). This allowed expression of either VVA0326-GFP or VVA0328-GFP coding region under control of the inducible *lac* promoter. All constructs were transformed into JM109 and the localization of VVA0326 and VVA0328 examined by fluorescence microscopy. The panels were photographed with an epifluorescence microscope with a normal light source to reveal the shape of the bacteria and with an excitation light equipped with a green filter set to observe the location of fluorescence in relation to the cell as a whole.

10. NanoOrange staining

A 0.5-μl portion of a Nano-Orange stock solution (Molecular Probes) was added to 10 μl of a live bacterial culture on a microscopic slide. Samples on the slide were then mixed with 10 to 20 ml of 30% polyvinylpyrrolidone (Sigma Chemical Co., St. Louis, Mo.) and covered with a coverslip. Polyvinylpyrrolidone was used for mounting both to reduce convection and to serve as a cryoprotectant, which allowed storage of slides for 1 to 2 weeks in a freezer. After waiting 10 to 15 min for staining to occur, I examined the slide at a magnification of $\times$1,000 with an epifluorescence microscope equipped with a blue filter set (excitation, wavelength, 490 nm; emission wavelength, 520 nm).

11. Multiple sequence alignment and phylogenetic estimation

Neighbor-Joining (NJ) trees built with the deduced amino acid sequences for GGDEF and EAL proteins were done by CLUSTAL W 1.81 (Thompson *et al.*, 1994). Default substitution matrix (Gonnet) was used for alignments, and the positions with gaps were excluded in the tree construction by complete deletion. The resultant trees

were constructed by Poisson correction model of MEGA3 program (Kumar *et al.*, 2004) and 1000 replications of bootstrap sampling were performed for each analysis.

Result

1. Bioinformatic analysis of the virulence-associated island

1-1. BLAST analysis and HMM searches

To understand the functional roles of these genes in the virulence-associated island, BLAST (Basic Local Alignment Search Tool) analysis of the sequence and HMM-profile (hidden Markov model based profiles) searching of the motifs were performed. As shown in Fig. 1, the genomic island of approximately 27 kb in length contains a typical type I secretion pathway (VVA0332 to VVA0334) downstream to the RtxL gene. The annotated functions of these genes are listed in Table 4. VVA0332 was annotated as a HlyB-like inner membrane traffic ATPase (with 26% a.a. sequence identity and 48% a.a. sequence similarity); VVA0333 is an HlyD-like inner membrane protein that is suggested to bridge to the outer membrane (like HlyD with 20% identity and 45% similarity) and VVA0334, an TolC-like outer membrane protein (like TolC with 20% identity and 41% similarity).

On the other end of the island, a VieSA like two component system gene cluster was found. It is composed of one sensor (VVA0329) with 36% identity and 50% similarity to VcVieS, two response regulators, VVA0325 with 25% identity and 49% similarity to VieA and VVA0327 with 36% identity and 56% similarity to VieA, and two novel signaling proteins, GGDEF- and EAL- containing protein (VVA0326, VVA0328). Analysis of the functional domains of the signal transduction system revealed two transmembrane domains (TM) in either VVA0329 or VVA0326 (Fig. 2). Topology analysis showed that they are located in the inner membrane and pass through the membrane twice. The cleavage site (CleavI) which could be recognized

was also identified. VVA0329 is an unorthodox (ITRO-type) sensor kinase containing histidine kinase domain (I, HATPase_c), histidne kinase A phosphoaccepter domain (T, HisKA), response regulator receiver domain(R, Response_reg) and histidine-containing phosphotransfer domain (O, Hpt). VVA0326 is a novel signaling protein with a GGDEF domain. Another two proteins (VVA0325 and VVA0327) which were predicted as response regulators contain receiver domain and a LuxR type HTH domain. The fifth member, VVA0328, of the signal transduction gene cluster encodes also a response regulator contain a receiver domain, however, with an EAL domain.

1-2. Interspecies comparison

Comparative analysis of the gene clusters containing either of RtxL (VVA0330), VvRtxA (VVA1030), or VcRtxA, revealed a type I secretion pathway gene cluster nearby (Fig. 3A). Besides the orthologous genes between VcRtxA and VvRtxA, sharing about 80–90% identical throughout most regions of the toxins (Sheahan *et al.*, 2004), the type I secretion pathway gene cluster downstream of them (VVA1031 to VVA1036 and VC1450 to VC1446) appears to be a homologous one. However, the RtxL and the downstream type I secretion pathway gene cluster have no significant similarity found to VVA1030-VVA1036 and VC1451-1446, and VVA0334, predicted as TolC like, is also dissimilar to the RtxB-like .

On analysis of the signaling transduction clusters upstream the RtxL, the two component system (VVA0326 to VVA0329, named as VvVieSA1) has a paralogous gene cluster (VVA0647 to VVA0651, named as VvVieSA2) (Fig. 3B). Besides, some interesting properties were found: VVA0327 and VVA0328 share a certain degree of homology with VieA sequence of *V. cholerae.* Different from the VieSAB of *V. cholerae* (named VcVieSAB), no VieB homolog was identified. The properties were

also found in the VieSA cluster of *V. parahaemolyticus* (VpVieSA). The percentage of identity and similarity between these four gene clusters were shown in Table 5, supporting the correlation: the VvVieSA1 is more similar to VpVieSA and VvVieSA2 is more like VcVieSA.

However, no homologous genes nearby the virulence-associated island were found comparing to another genome even though the homologous VieSA gene clusters were found in, *V. cholerae* and *V. parahaemolyticus*.

1-3. Sequence analysis of RtxL

To know whether the glycine-rich repeats or the β-sheet pore, the major feature of RTX and autotransporter respectively, exists in RtxL using primary sequence search in the software RADAR **(R**apid **A**utomatic **D**etection and **A**lignment of **R**epeats). Unexpectedly, unlike numerous small repeats in the typical RTX protein, three repeats of 539 aa in length were found (Fig. 4). The three regions start from 677 aa to 1216 aa, 1217 aa to 1755 aa, and 1756 aa to 2293 aa. Except for the consensus four cysteine at the 3888, 3985, 3998 and 4133 aa residues, neither signal peptide nor β-sheet sequence was found.

2. Mutagenesis of the VVA0326, VVA0328 and *rtxL*

2-1. Construction of the VVA0326, VVA0328 and *rtxL* mutants

VVA0326, VVA0328, and RtxL were chosen for mutant construction for further identifying the function in *Vibrio vulnificus* YJ016. As shown in Fig. 5A, the deleted DNA fragments included respectively about 500-bp in VVA0326, 800-bp in VVA0328 and 800-bp in RtxL. As shown in Fig. 5B, 1000-, 1600- and 1300-bp signals were

obtained respectively in the mutants while using the corresponding probes. This confirmed the expected deletion in each of VVA0326, VVA0328, and RtxL. The VVA0326$^-$VVA0328$^-$ double mutant was also constructed in order to demonstrate if the ORFs encode functionally coordinated proteins.

2-2. Characterization of VVA0326$^-$, VVA0328$^-$ and *rtxL*$^-$ mutants

2-2-1. Analysis of the bacterial growth

Both VVA0326$^-$ and VVA0326$^-$VVA0328$^-$ mutant displayed smaller colony morphology on LB agar while compared to the wild type strain. In addition growth rate of the two mutants appeared to be slower in log phase comparing to that of wild type strain in LB broth (Fig. 6A). However, no significant difference was found when the broth in either 2 h or 4 h plated on LB agar plate for the colony forming units (CFU), indicating that growth rate is not a major factor to confer the small colony (Fig. 6B).

2-2-2. Cytotoxicity analysis of *rtxL*$^-$ mutant

The monolayer of the cell was infected with the wild type and *rtxL*$^-$ bacteria at a multiplicity of infection (MOI) of 10. After incubation at 37°C for 2 h and 4 h, the cytotoxicity was determined by measuring the activity of the lactate dehydrogenase (LDH) in the supernatant from the dead cells. As shown in Fig. 7, the percentages of cytotoxicity of wild-type and *rtxL*$^-$ bacteria appeared to be similar at either 2 h or 4 h.

2-2-3. Morphotypic analysis of the mutants by Congo-Red and CAS agar plates

It has been reported in *Salmonella* Typhimurium that changes in the bacterial surface could be detected when the bacteria were plated on Congo-Red plate (Romling *et al.*, 2000). As shown in Fig. 8A, no obvious difference could be found

when either of the mutants plated on the plates incubated either at 37°C or 30°C.

When the bacteria were cultured on CAS agar plate at 30°C, VVA0326$^-$ and VVA0326$^-$ VVA0328$^-$ mutants appeared to grow better than wild type and an apparent yellow color was found around the colonies after the plates were incubated for 48 h (Fig. 8B). However, no differences could be identified when the bacteria were incubated at 37°C. In contrast, VVA0328$^-$ mutant appeared to have a poor growth rate on CAS plate comparing with wild type at 30°C.

2-2-4. Analysis of polysaccharide of plate grown cells

As shown in Fig. 9, analysis of the polysaccharide contents revealed that, in the 12.5% running gel detected with silver stain, VVA0326$^-$ and VVA0326$^-$VVA0328$^-$ mutants show less intensity than that of wild type.

2-2-5. Scanning electron microscopy of plate grown cells

Electron microscopy analysis of wild type and the derived mutant strains revealed a slight difference of the intercellular distance between the bacteria of wild type and VVA0326$^-$ (Fig. 10).

2-2-3. Deletion of GGDEF domain in VVA0326 increased the bacterial swimming motility

On a 0.3% soft agar, VVA0326$^-$ and VVA0326$^-$VVA0328$^-$ mutants showed a obvious increase of swimming motility, comparing to wild type at either 37°C or 30°C. No apparent affect on the bacterial motility could be observed in either VVA0328$^-$ or *rtxL*$^-$ mutants (Fig. 11).

3. Subcellular localization of the recombinant VVA0326 and VVA0328 proteins in *E.coli*

The plasmids pVVA0326-GFP and pVVA0328-GFP which carrying

VVA0326-GFP and VVA0328-GFP translational fusion constructs were transformed respectively into *E. coli* JM109 to examine the subcellular location of the two proteins. The expression pattern of the bacteria containing the pGFP, pVVA0326-GFP, and pVVA0328-GFP respectively were shown in Fig. 12B. An obvious protein expression pattern of VVA0328-GFP was found, however no apparent expression pattern of VVA0326-GFP was found. Phenotypes of the bacteria carrying either VVA0326-GFP or VVA0328-GFP appeared to be similar to those of the bacteria harboring VVA0326 (pGGDEF) and VVA0328 (pEAL) implying that the activities of the two proteins are not affected by fusing to GFP. As shown in Fig. 13A-2, E. coli JM109 [pGFP] expressed green fluorescence all over the cell. Whereas, the green fluorescence displayed by the bacteria carrying VVA0326-GFP appeared to be localized on the membrane. Interestingly, VVA0328-GFP protein was also located at the pole and mostly present at one pole in bacteria (Fig. 13B-2 and 13C-2). We attempted to orient this pole with respect to the position of the flagella, but the methods that I utilized for flagellum staining did not give reliable results (Grossart *et al.*, 2000).

4. Genome-wide analysis of GGDEF- and EAL- domain containing proteins

4-1. Most bacteria contain GGDEF- and EAL- proteins

Over 220 complete microbial genomes currently available allow obtaining accurate counts of the number of GGDEF- and EAL- proteins. As shown in Table 6, analysis of the selected 50 bacterial genomes revealed several interesting trends: Although the genome size of *Aquifex aeolicus* VF5 is rather small, it has more of the GGDEF and EAL proteins than those of the larger bacteria such as *Shigella* and *Yersinia*. *Streptomyces coelicolor* which have the largest genome carry even less of

the proteins. The notion indicated that the number of the GGDEF and EAL proteins could not be correlated with the bacterial genome size. The bacteria, *Vibrio* and *Pseudomona*, which grow in a variety of environmental habitats, have the most number of the GGDEF and EAL proteins implying the involvement of the signaling system with their capabilities to encounter the highly changing environment. I also employ a search of the major cellulose gene bcsB and flagellin domain among the genomes. The results indicated that not all of the genomes containing genes encoding GGDEF- and EAL- proteins also carry cellulose synthesis genes. This suggested that another biological functional role exists other than involvement of cellulose synthesis reported previously (Ross *et al.*, 1990). The most recent study has shown that *morA* which encodes a GGDEF-EAL protein restricted *fliC* expression and hence affect flagellar development in *P. aeruginosa* (Choy *et al.*, 2004). A search of the flagellin domain among the genomes was also analyzed. A significant correlation between the flagellin gene and the gene encoding GGDEF- and EAL- proteins was found. (Chi-squre, d.f.=1, p-value = 0.0002753). This result confirmed the possibility I mentioned above.

4-2. Evolutionary analysis of the GGDEF- and EAL- proteins

Interestingly, as shown in Table 6, a great proportion of GGDEF-EAL proteins were found suggesting an evolutionary relationship between the two domains. To address the evolutionary relationship of GGDEF- and EAL- proteins, phylogenetic analysis was performed.

4-2-1. Organization of genes encoding GGDEF- and EAL- proteins

Analysis of 1601 GGDEF- and 1016 EAL- proteins collected in the Pfam database (Version 17.0) revealed 622 proteins containing both GGDEF and EAL

domains. It is interesting to note that only two types of domain organization could be identified and the distance between the two domains in the proteins appeared to be conserved. As shown in Fig. 14, 606 of the proteins were classified into A type, the GGDEF was about 15 aa in front of EAL, and 16 were the B type, the GGDEF was about 170 aa rear to EAL. The A type protein was found in the genome of the ancient bacteria *Aquifex aeolicus* VF5 implying that the A type was the ancestor evolved age ago.

4-2-2. Phylogenetic trees of the GGDEF and EAL proteins of *V. vulnificus* YJ016

A whole genome analysis of the annotated 4958 proteins of *V. vulnificus* using HMMER revealed 63 GGDEF and 31 EAL proteins, and 18 of them carry both domains. In order to study whether the GGDEF-EAL proteins were aroused from a common ancestor through gene duplication event or assemblies of GGDEF and EAL domains from various proteins through recombination, phylogenetic tree respectively for 32 EAL proteins and 63 GGDEF protein were constructed using neighbor-joining analysis. As shown in Fig.15, except for a few GGDEF-EAL proteins (Q7MQD8 in GGDEF tree, and Q7MJM1, Q7MBT4, Q7MHB9 and Q7MQD8 in EAL tree), most cluster together. The result supported the assumption, GGDEF-EAL proteins come from the same ancestor. Besides, comparing to domain structure of the proteins, several duplication events were found in the phylogenetic trees implying that it is one reason to cause multi-copy of GGDEF- and EAL- proteins (Fig. 16).

4-2-3. The GGDEF domain evolved faster than EAL domain

Eighteen proteins containing both GGDEF and EAL domains from *V. vulnificus* YJ016 were collected and analyzed. Multiple sequence alignment of the deduced amino acid sequences of either GGDEF, EAL or GGDEF-EAL domains using

CLUSTAL W was performed and subsequently subject to the neighbor-joining analysis for tree construction using MEGA program. As depicted in Fig. 17, the tree topology of EAL domain is very similar to GGDEF-EAL domain with respect to the positions of common sequences. Subsequent to this, five clades (congruent monophyletic groups) compose of 11 GGDEF-EAL pairs designated as clades A to E respectively were identified. However, comparing the EAL tree with GGDEF tree, any of the clades could not be found except clade A. It implies that two domains have no significant co-evolutionary rate even though they maybe come from the same ancestor by duplication. While comparing the domain sequences, the similarities obtained from GGDEF domains appeared to be much less than that obtained from EAL domains. So, the respective p distance of the two domains from the 18 proteins measured by Mega program were 0.755 and 0.681 respectively for GGDEF and EAL domains, implying the GGDEF domain evolved faster than EAL domain.

Discussion

1. Functional analysis of RtxL

No cytotoxicity was found when comparing RtxL$^-$ with wild type strain. The typical feature of RTX toxin family, including acidic glycine-rich nonapeptide repeats, hydrophobic region and posttranslational maturation, was not found in the gene product except for a gene cluster encoding a type I secretion pathway at *rtxL* downstream. This implies the presence of a novel property in the large protein.

Unlike the small repeats (12 to 18 aa) in RTX proteins, three long repeats of 539 aa in length were found in RtxL. Sequence search in Genebank revealed several large proteins, such as DP0561 of *Desulfotalea psychrophila* LSv54, Ecs0542 of *Escherichia coli* O157:H7 and t4166 of *Salmonella enterica* subsp Typhi Ty2, which share 20% to 40% identities to the N-termianl 1-2400 aa of RtxL. All of the large protein encoding gene appeared to be linked with a gene cluster of type I secretion pathway. Like RtxL, they are also composed of long repetitive peptides with differences in sequence and number. However, none of the proteins have been functionally characterized.

2. Functional analysis of VVA0326 and VVA0328

Both GGDEF and EAL domains have been reported to contribute to cyclic di-GMP metabolism, whereby the GGDEF domain represents the diguanylate cyclase, while EAL, most probably, represents the diguanylate phosphodiesterase (Ausmees *et al.*, 2001; Simm *et al.*, 2004; Tal *et al.*, 1998). Analysis of the gene organization revealed that VVA0328 together with VVA0326 are likely regulated by the same

promoter. In addition, VVA0326-GFP or VVA0328-GFP proteins tended to localize at the cell poles in a manner similar to that observed earlier for methylaccepting chemotaxis proteins (MCPs) (Sourjik and Berg, 2000). Hence I believe that they are expressed concordantly. However, only the GGDEF- containing VVA0326 appeared to be required for the bacterial swimming motility. This could be explained that VVA0326 and VVA0328 are expressed in a general culture condition under a same promoter, but only VVA0326 protein exerts a cyclase activity. Whereas, VVA0328 protein function must be activated upon signal receiving in a specific environment by its response regulator domain.

In the previous study, overdose of HDTMA (hexadecyltrimethyl ammonium bromide) is toxic to Gram-positive and a few Gram-negative bacteria (Schwyn and Neilands, 1987). The difference of susceptibility was attributed to the dissimilar surface structure. VVA0326^{-}, the GGDEF mutant appeared to be resistant to HDTMA at 30°C. While VVA0328^{-}, the EAL mutant was sensitive to HDTMA suggesting the surface structure altered by deletion of either GGDEF or EAL. SEM (scanning electronic microscope) analysis is being carried out to assess the effect of either deletion on the bacterial surface structure.

To further address how these two proteins, VVA0326 and VVA0328, affect the swimming ability, two hypotheses were suggested. One is that the synthesis of flagella is affected directly, and the other is that the structure of exopolysaccharide is influenced and affects motility indirectly. Based on the results of CAS plate, exopolysaccharide could be a component changed by VVA0326 and VVA0328 to affect swimming ability. However, the possibility of flagellar alteration still can not be excluded.

3. Evolutionary analysis of GGDEF- and EAL- proteins

The presence of so many GGDEF- and EAL- proteins in a bacterial genome raises the question of how the readout specificity of parallel signaling pathways might be achieved if all of these converge in a central, freely diffusible cellular pool of cyclic di-GMP. Could specificity be achieved through spatial organization of diguanylate cyclase, in response to different signals, to locally control the activity of surface modulating factors? Aside from cellulose synthase, what are the downstream targets of cyclic di-GMP and how would these interact with the diverse processes? As shown in Table 6, not all bacteria which have GGDEF- and EAL- containing proteins also carry the genes encoding cellulose synthesis gene. The result suggested that other downstream targets are present under the regulation of cyclic di-GMP. A recent report has shown that MorA, a GGDEF-EAL protein, restricted fliC expression and hence affects flagellar development in *P. aeruginosa* (Choy et al., 2004). A significant correlation between flagellin and GGDEF- and EAL- containing proteins was found in the genome analysis shown in Table 7. This suggested that bacterial flagellar biosynthesis is under control by the cellular level of cyclic di-GMP.

Many proteins contain both GGDEF- and EAL- domains, like the six proteins (DGC1, DGC2, DGC3, PDE1, PDE2 and PDE3) reported in *Acetobacter xylinum*. Three of them (DGC1, DGC2 and DGC3) were shown to be diguanylate cyclases and the other three (PDE1, PDE2 and PDE3) were phosphodiesterase. The enzyme activities of the proteins, ScrC, MbaA, RocS, FimX, and MorA, which also contain both domains.

The molecular modeling for nucleotide cyclase activity of the GGDEF domain (Pei and Grishin, 2001) and the structural analysis of the crystallized GGDEF domain of PleD allowed to confirm the catalytic mechanism (Chan *et al.*, 2004).

Nevertheless, no structural analysis of the EAL domain is available despite of its requirement for breakdown of cyclic-di-GMP in vivo (Simm *et al.*, 2004).

In this study, A type is considered to be the ancestor exist long time ago, because most both GGDEF- and EAL- containing proteins are this type and it is also found in the ancient bacteria *Aquifex aeolicus* VF5. According to the phylogenetic analysis of GGDEF- and EAL- containing proteins in *Vibrio vulnificus* YJ016, most of the GGDEF-EAL proteins were clustered and several duplication events were found indicating most GGDEF- and EAL- containing proteins increase from the same ancestor by gene duplication. The homology was kept in the GGDEF-EAL proteins, implying the two domains still retain respectively enzymatic activity for an inverse regulation of the cyclic di-GMP level. However, how do the two enzymes coordinate the opposite function? A model is proposed: both domains in such a protein must be important equally and have respective functions. One of them is constitutively expressed, while activity of the other enzyme could be activated only upon an environmental stimulation, possibly resulting in a conformational change of the protein. I believed that this is an effective strategy for bacteria to control the level of cyclic di-GMP for appropriate signal transduction.

As shown in fig 13, the phylogenetics trees of GGDEF- and EAL- containing proteins revealed one group of GGDEF- proteins or EAL- proteins on the treetop suggesting that the single domain containing proteins arised earlier than the GGDEF-EAL proteins. Similar results were obtained when other bacteria including *Aquifex aeolicus* VF5, *Escherichia*, *Salmonella* and *Pseudomona,* were selected for comparison (data not shown). This suggested that the GGDEF-EAL proteins arised from assemble of GGDEF and EAL domains.

The analysis showed that the two domains exerted different evolutionary rate even though they likely coevolved by duplication. This is likely that sequence

conservation is more restricted for EAL domain. The relatively variable sequence of GGDEF domain implies a high adaptation capability.

It is clear that we are only just beginning to understand the role of GGDEF- and EAL- proteins in bacteria. However, more and more virulence associated roles of them such as biofilm formation, morphogenesis, exopolysaccharide biosynthesis and motility of the bacteria were reported. These studies appear to offer attractive targets for antimicrobials by interfering with synthesis, breakdown and recognition of cyclic di-GMP (Karaolis *et al.*, 2005).

Reference

Aldridge, P., and Jenal, U. (1999) Cell cycle-dependent degradation of a flagellar motor component requires a novel-type response regulator. *Mol Microbiol* **32**: 379-391.

Aldridge, P., Paul, R., Goymer, P., Rainey, P., and Jenal, U. (2003) Role of the GGDEF regulator *PleD* in polar development of *Caulobacter crescentus*. *Mol Microbiol* **47**: 1695-1708.

Ausmees, N., Mayer, R., Weinhouse, H., Volman, G., Amikam, D., Benziman, M., and Lindberg, M. (2001) Genetic data indicate that proteins containing the GGDEF domain possess diguanylate cyclase activity. *FEMS Microbiol Lett* **204**: 163-167.

Baumann, U., Wu, S., Flaherty, K.M., and McKay, D.B. (1993) Three-dimensional structure of the alkaline protease of *Pseudomonas aeruginosa*: a two-domain protein with a calcium binding parallel beta roll motif. *Embo J* **12**: 3357-3364.

Bendtsen, J.D., Nielsen, H., von Heijne, G., and Brunak, S. (2004) Improved prediction of signal peptides: SignalP 3.0. *J Mol Biol* **340**: 783-795.

Biosca, E.G., Fouz, B., Alcaide, E., and Amaro, C. (1996) Siderophore-mediated iron acquisition mechanisms in *Vibrio vulnificus* biotype 2. *Appl Environ Microbiol* **62**: 928-935.

Boardman, B.K., and Satchell, K.J. (2004) *Vibrio cholerae* strains with mutations in an atypical type I secretion system accumulate RTX toxin intracellularly. *J Bacteriol* **186**: 8137-8143.

Boehm, D.F., Welch, R.A., and Snyder, I.S. (1990) Calcium is required for binding of *Escherichia coli* hemolysin (HlyA) to erythrocyte membranes. *Infect Immun* **58**: 1951-1958.

Boles, B.R., and McCarter, L.L. (2002) *Vibrio parahaemolyticus scrABC*, a novel operon affecting swarming and capsular polysaccharide regulation. *J Bacteriol* **184**: 5946-5954.

Bomchil, N., Watnick, P., and Kolter, R. (2003) Identification and characterization of a *Vibrio cholerae* gene, *mbaA*, involved in maintenance of biofilm architecture. *J Bacteriol* **185**: 1384-1390.

Botsford, J.L. (1981) Cyclic nucleotides in procaryotes. *Microbiol Rev* **45**: 620-642.

Botsford, J.L., and Harman, J.G. (1992) Cyclic AMP in prokaryotes. *Microbiol Rev* **56**: 100-122.

Burrows, L.L., and Lo, R.Y. (1992) Molecular characterization of an RTX toxin determinant from *Actinobacillus suis*. *Infect Immun* **60**: 2166-2173.

Camilli, A., and Mekalanos, J.J. (1995) Use of recombinase gene fusions to identify *Vibrio cholerae* genes induced during infection. *Mol Microbiol* **18**: 671-683.

Chan, C., Paul, R., Samoray, D., Amiot, N.C., Giese, B., Jenal, U., and Schirmer, T. (2004) Structural basis of activity and allosteric control of diguanylate cyclase. *Proc Natl Acad Sci U S A* **101**: 17084-17089.

Chen, C.Y., Wu, K.M., Chang, Y.C., Chang, C.H., Tsai, H.C., Liao, T.L., Liu, Y.M., Chen, H.J., Shen, A.B., Li, J.C., Su, T.L., Shao, C.P., Lee, C.T., Hor, L.I., and Tsai, S.F. (2003) Comparative genome analysis of *Vibrio vulnificus*, a marine pathogen. *Genome Res* **13**: 2577-2587.

Choy, W.K., Zhou, L., Syn, C.K., Zhang, L.H., and Swarup, S. (2004) MorA defines a new class of regulators affecting flagellar development and biofilm formation in diverse *Pseudomonas* species. *J Bacteriol* **186**: 7221-7228.

de Lorenzo, V., and Timmis, K.N. (1994) Analysis and construction of stable phenotypes in gram-negative bacteria with Tn5- and Tn10-derived minitransposons. *Methods Enzymol* **235**: 386-405.

Donnenberg, M.S., and Kaper, J.B. (1991) Construction of an *eae* deletion mutant of enteropathogenic *Escherichia coli* by using a positive-selection suicide vector. *Infect Immun* **59**: 4310-4317.

Drenkard, E., and Ausubel, F.M. (2002) *Pseudomonas* biofilm formation and antibiotic resistance are linked to phenotypic variation. *Nature* **416**: 740-743.

Frey, J., Bosse, J.T., Chang, Y.F., Cullen, J.M., Fenwick, B., Gerlach, G.F., Gygi, D., Haesebrouck, F., Inzana, T.J., Jansen, R., and et al. (1993) *Actinobacillus pleuropneumoniae* RTX-toxins: uniform designation of haemolysins, cytolysins, pleurotoxin and their genes. *J Gen Microbiol* **139**: 1723-1728.

Fullner, K.J., and Mekalanos, J.J. (2000) In vivo covalent cross-linking of cellular actin by the *Vibrio cholerae* RTX toxin. *Embo J* **19**: 5315-5323.

Galperin, M.Y., Nikolskaya, A.N., and Koonin, E.V. (2001) Novel domains of the prokaryotic two-component signal transduction systems. *FEMS Microbiol Lett* **203**: 11-21.

Galperin, M.Y. (2004) Bacterial signal transduction network in a genomic perspective. *Environ Microbiol* **6**: 552-567.

Glaser, P., Sakamoto, H., Bellalou, J., Ullmann, A., and Danchin, A. (1988) Secretion of cyclolysin, the calmodulin-sensitive adenylate cyclase-haemolysin bifunctional protein of *Bordetella pertussis*. *Embo J* **7**: 3997-4004.

Gray, J.T., Fedorka-Cray, P.J., and Rogers, D.G. (1995) Partial characterization of a Moraxella bovis cytolysin. *Vet Microbiol* **43**: 183-196.

Gray, L.D., and Kreger, A.S. (1989) Detection of *Vibrio vulnificus* cytolysin in *V. vulnificus*-infected mice. *Toxicon* **27**: 439-464.

Grossart, H.P., Steward, G.F., Martinez, J., and Azam, F. (2000) A simple, rapid method for demonstrating bacterial flagella. *Appl Environ Microbiol* **66**:

3632-3636.

Guvener, Z.T., and McCarter, L.L. (2003) Multiple regulators control capsular polysaccharide production in *Vibrio parahaemolyticus*. *J Bacteriol* **185**: 5431-5441.

Hecht, G.B., and Newton, A. (1995) Identification of a novel response regulator required for the swarmer-to-stalked-cell transition in *Caulobacter crescentus*. *J Bacteriol* **177**: 6223-6229.

Hlady, W.G., Mullen, R.C., and Hopkin, R.S. (1993) *Vibrio vulnificus* from raw oysters. Leading cause of reported deaths from foodborne illness in Florida. *J Fla Med Assoc* **80**: 536-538.

Hlady, W.G., and Klontz, K.C. (1996) The epidemiology of *Vibrio* infections in Florida, 1981-1993. *J Infect Dis* **173**: 1176-1183.

Hoi, L., Larsen, J.L., Dalsgaard, I., and Dalsgaard, A. (1998) Occurrence of *Vibrio vulnificus* biotypes in Danish marine environments. *Appl Environ Microbiol* **64**: 7-13.

Hsueh, P.R., Lin, C.Y., Tang, H.J., Lee, H.C., Liu, J.W., Liu, Y.C., and Chuang, Y.C. (2004) *Vibrio vulnificus* in Taiwan. *Emerg Infect Dis* **10**: 1363-1368.

Huang, B., Whitchurch, C.B., and Mattick, J.S. (2003) FimX, a multidomain protein connecting environmental signals to twitching motility in *Pseudomonas aeruginosa*. *J Bacteriol* **185**: 7068-7076.

Johnson, D.E., Calia, F.M., Musher, D.M., and Goree, A. (1984) Resistance of *Vibrio vulnificus* to serum bactericidal and opsonizing factors: relation to virulence in suckling mice and humans. *J Infect Dis* **150**: 413-418.

Juncker, A.S., Willenbrock, H., Von Heijne, G., Brunak, S., Nielsen, H., and Krogh, A. (2003) Prediction of lipoprotein signal peptides in Gram-negative bacteria. *Protein Sci* **12**: 1652-1662.

Karaolis, D.K., Rashid, M.H., Chythanya, R., Luo, W., Hyodo, M., and Hayakawa, Y. (2005) c-di-GMP (3'-5'-cyclic diguanylic acid) inhibits *Staphylococcus aureus* cell-cell interactions and biofilm formation. *Antimicrob Agents Chemother* **49**: 1029-1038.

Kohler, T., Curty, L.K., Barja, F., van Delden, C., and Pechere, J.C. (2000) Swarming of *Pseudomonas aeruginosa* is dependent on cell-to-cell signaling and requires flagella and pili. *Journal of Bacteriology* **182**: 5990-5996.

Koronakis, V., Cross, M., Senior, B., Koronakis, E., and Hughes, C. (1987) The secreted hemolysins of *Proteus mirabilis*, *Proteus vulgaris*, and *Morganella morganii* are genetically related to each other and to the alpha-hemolysin of *Escherichia coli*. *J Bacteriol* **169**: 1509-1515.

Kraig, E., Dailey, T., and Kolodrubetz, D. (1990) Nucleotide sequence of the

leukotoxin gene from *Actinobacillus actinomycetemcomitans*: homology to the alpha-hemolysin/leukotoxin gene family. *Infect Immun* **58**: 920-929.

Kumar, S., Tamura, K., and Nei, M. (2004) MEGA3: Integrated software for Molecular Evolutionary Genetics Analysis and sequence alignment. *Brief Bioinform* **5**: 150-163.

Lally, E.T., Hill, R.B., Kieba, L.R., and Korostoff, J. (1999) The interaction between RTX toxins and target cells. *Trends in Microbiology* **7**: 356-361.

Lee, S.H., Angelichio, M.J., Mekalanos, J.J., and Camilli, A. (1998) Nucleotide sequence and spatiotemporal expression of the *Vibrio cholerae vieSAB* genes during infection. *J Bacteriol* **180**: 2298-2305.

Lee, S.H., Butler, S.M., and Camilli, A. (2001) Selection for in vivo regulators of bacterial virulence. *Proc Natl Acad Sci U S A* **98**: 6889-6894.

Lin, W., Fullner, K.J., Clayton, R., Sexton, J.A., Rogers, M.B., Calia, K.E., Calderwood, S.B., Fraser, C., and Mekalanos, J.J. (1999) Identification of a *Vibrio cholerae* RTX toxin gene cluster that is tightly linked to the cholera toxin prophage. *Proc Natl Acad Sci U S A* **96**: 1071-1076.

Locht, C. (1999) Molecular aspects of *Bordetella pertussis* pathogenesis. *Int Microbiol* **2**: 137-144.

Ludwig, A., Jarchau, T., Benz, R., and Goebel, W. (1988) The repeat domain of *Escherichia coli* haemolysin (HlyA) is responsible for its Ca2+-dependent binding to erythrocytes. *Mol Gen Genet* **214**: 553-561.

McCarter, L.L., and Silverman, M. (1987) Phosphate regulation of gene expression in *Vibrio parahaemolyticus*. *J Bacteriol* **169**: 3441-3449.

McPherson, V.L., Watts, J.A., Simpson, L.M., and Oliver, J.D. (1991) Physiological effects of the lipopolysaccharide of *Vibrio vulnificus* on mice and rats. *Microbios* **67**: 141-149.

Merkel, T.J., Barros, C., and Stibitz, S. (1998) Characterization of the *bvgR* locus of *Bordetella pertussis*. *J Bacteriol* **180**: 1682-1690.

Miller, J.F., Mekalanos, J.J., and Falkow, S. (1989) Coordinate regulation and sensory transduction in the control of bacterial virulence. *Science* **243**: 916-922.

Mizuno, T. (1998) His-Asp phosphotransfer signal transduction. *J Biochem (Tokyo)* **123**: 555-563.

O'Toole, G.A., and Kolter, R. (1998) Flagellar and twitching motility are necessary for *Pseudomonas aeruginosa* biofilm development. *Mol Microbiol* **30**: 295-304.

Okada, K., Iida, T., Kita-Tsukamoto, K., and Honda, T. (2005) Vibrios commonly possess two chromosomes. *J Bacteriol* **187**: 752-757.

Oliver, J.D., Wear, J.E., Thomas, M.B., Warner, M., and Linder, K. (1986) Production of extracellular enzymes and cytotoxicity by *Vibrio vulnificus*. *Diagn*

Microbiol Infect Dis **5**: 99-111.

Paul, R., Weiser, S., Amiot, N.C., Chan, C., Schirmer, T., Giese, B., and Jenal, U. (2004) Cell cycle-dependent dynamic localization of a bacterial response regulator with a novel di-guanylate cyclase output domain. *Genes Dev* **18**: 715-727.

Pei, J., and Grishin, N.V. (2001) GGDEF domain is homologous to adenylyl cyclase. *Proteins* **42**: 210-216.

Rashid, M.H., Rajanna, C., Ali, A., and Karaolis, D.K. (2003) Identification of genes involved in the switch between the smooth and rugose phenotypes of *Vibrio cholerae*. *FEMS Microbiol Lett* **227**: 113-119.

Romling, U., Rohde, M., Olsen, A., Normark, S., and Reinkoster, J. (2000) AgfD, the checkpoint of multicellular and aggregative behaviour in *Salmonella typhimurium* regulates at least two independent pathways. *Mol Microbiol* **36**: 10-23.

Ross, P., Mayer, R., Weinhouse, H., Amikam, D., Huggirat, Y., Benziman, M., de Vroom, E., Fidder, A., de Paus, P., Sliedregt, L.A., and et al. (1990) The cyclic diguanylic acid regulatory system of cellulose synthesis in *Acetobacter xylinum*. Chemical synthesis and biological activity of cyclic nucleotide dimer, trimer, and phosphothioate derivatives. *J Biol Chem* **265**: 18933-18943.

Sambrook, J., and Russell, D.W. (2001) *Molecular Cloning: a laboratory manual-3rd edition.*: Cold Spring Harbor Laboratory Press, Cold Spring Harbor, New York.

Schmidt, H., Kernbach, C., and Karch, H. (1996) Analysis of the EHEC *hly* operon and its location in the physical map of the large plasmid of enterohaemorrhagic *Escherichia coli* O157:H7. *Microbiology-Uk* **142**: 907-914.

Schwyn, B., and Neilands, J.B. (1987) Universal chemical assay for the detection and determination of siderophores. *Anal Biochem* **160**: 47-56.

Shao, C.P., and Hor, L.I. (2000) Metalloprotease is not essential for *Vibrio vulnificus* virulence in mice. *Infect Immun* **68**: 3569-3573.

Sheahan, K.L., Cordero, C.L., and Satchell, K.J. (2004) Identification of a domain within the multifunctional *Vibrio cholerae* RTX toxin that covalently cross-links actin. *Proc Natl Acad Sci U S A* **101**: 9798-9803.

Simm, R., Morr, M., Kader, A., Nimtz, M., and Romling, U. (2004) GGDEF and EAL domains inversely regulate cyclic di-GMP levels and transition from sessility to motility. *Mol Microbiol* **53**: 1123-1134.

Soncini, F.C., and Groisman, E.A. (1996) Two-component regulatory systems can interact to process multiple environmental signals. *J Bacteriol* **178**:

6796-6801.

Sourjik, V., and Berg, H.C. (2000) Localization of components of the chemotaxis machinery of *Escherichia coli* using fluorescent protein fusions. *Mol Microbiol* **37**: 740-751.

Spiers, A.J., Kahn, S.G., Bohannon, J., Travisano, M., and Rainey, P.B. (2002) Adaptive divergence in experimental populations of *Pseudomonas fluorescens*. I. Genetic and phenotypic bases of wrinkly spreader fitness. *Genetics* **161**: 33-46.

Spiers, A.J., Bohannon, J., Gehrig, S.M., and Rainey, P.B. (2003) Biofilm formation at the air-liquid interface by the *Pseudomonas fluorescens* SBW25 wrinkly spreader requires an acetylated form of cellulose. *Mol Microbiol* **50**: 15-27.

Stanley, P., Koronakis, V., and Hughes, C. (1998) Acylation of *Escherichia coli* hemolysin: a unique protein lipidation mechanism underlying toxin function. *Microbiol Mol Biol Rev* **62**: 309-333.

Stock, J.B., Ninfa, A.J., and Stock, A.M. (1989) Protein phosphorylation and regulation of adaptive responses in bacteria. *Microbiol Rev* **53**: 450-490.

Strathdee, C.A., and Lo, R.Y. (1987) Extensive homology between the leukotoxin of *Pasteurella haemolytica* A1 and the alpha-hemolysin of *Escherichia coli*. *Infect Immun* **55**: 3233-3236.

Strom, M.S., and Paranjpye, R.N. (2000) Epidemiology and pathogenesis of *Vibrio vulnificus*. *Microbes Infect* **2**: 177-188.

Tal, R., Wong, H.C., Calhoon, R., Gelfand, D., Fear, A.L., Volman, G., Mayer, R., Ross, P., Amikam, D., Weinhouse, H., Cohen, A., Sapir, S., Ohana, P., and Benziman, M. (1998) Three *cdg* operons control cellular turnover of cyclic di-GMP in *Acetobacter xylinum*: genetic organization and occurrence of conserved domains in isoenzymes. *J Bacteriol* **180**: 4416-4425.

Taylor, R.K., Manoil, C., and Mekalanos, J.J. (1989) Broad-host-range vectors for delivery of TnphoA: use in genetic analysis of secreted virulence determinants of *Vibrio cholerae*. *J Bacteriol* **171**: 1870-1878.

Thompson, J.D., Higgins, D.G., and Gibson, T.J. (1994) CLUSTAL W: improving the sensitivity of progressive multiple sequence alignment through sequence weighting, position-specific gap penalties and weight matrix choice. *Nucleic Acids Res* **22**: 4673-4680.

Tischler, A.D., Lee, S.H., and Camilli, A. (2002) The *Vibrio cholerae vieSAB* locus encodes a pathway contributing to cholera toxin production. *J Bacteriol* **184**: 4104-4113.

Tischler, A.D., and Camilli, A. (2004) Cyclic diguanylate (c-di-GMP) regulates *Vibrio cholerae* biofilm formation. *Mol Microbiol* **53**: 857-869.

von Heijne, G. (1992) Membrane protein structure prediction. Hydrophobicity analysis and the positive-inside rule. *J Mol Biol* **225**: 487-494.

Welch, R.A. (1987) Identification of two different hemolysin determinants in uropathogenic *Proteus* isolates. *Infect Immun* **55**: 2183-2190.

Welch, R.A. (2001) RTX toxin structure and function: a story of numerous anomalies and few analogies in toxin biology. *Curr Top Microbiol Immunol* **257**: 85-111.

West, A.H., and Stock, A.M. (2001) Histidine kinases and response regulator proteins in two-component signaling systems. *Trends Biochem Sci* **26**: 369-376.

Whitfield, C., and Roberts, I.S. (1999) Structure, assembly and regulation of expression of capsules in *Escherichia coli*. *Mol Microbiol* **31**: 1307-1319.

Wright, A.C., Miceli, G.A., Landry, W.L., Christy, J.B., Watkins, W.D., and Morris, J.G., Jr. (1993) Rapid identification of *Vibrio vulnificus* on nonselective media with an alkaline phosphatase-labeled oligonucleotide probe. *Appl Environ Microbiol* **59**: 541-546.

Zogaj, X., Nimtz, M., Rohde, M., Bokranz, W., and Romling, U. (2001) The multicellular morphotypes of *Salmonella typhimurium* and *Escherichia coli* produce cellulose as the second component of the extracellular matrix. *Mol Microbiol* **39**: 1452-1463.

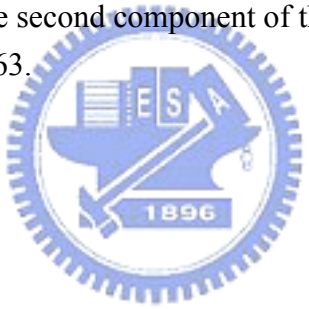

Tables

Table 1. Bacterial strains used and constructed in this study

Strains	Genotypes or relevant properties	Reference or source
E. coli		
NovaBlue (DE3)	*endA1 hsdR17*($rk_{12}^{-}mk_{12}^{+}$) *supE44 thi-1 recA1 gyrA96 relA1 lac*[F′ *pro AB lac*^{q}Z△M15:: Tn*10*](DE3);Tet^{r}	Novagen
JM109	*RecA1 supE44 endA1 hsdR17 gyrA96 rolA1 thi △ (lac-proAB)*	Laboratory stock
S17-1 λ *pir*	Tp^{r} Sm^{r} *recA, thi, pro, hsdR*$^{-}$*M*$^{+}$ [RP4-2-Tc::Mu:Km^{r}Tn*7*] (*pir*)	(de Lorenzo and Timmis, 1994)
ICC188 λ *pir*	△*(ara-leu) araD* △*lac×74 galE galK phoA20*	(Taylor *et al.*, 1989)
V.vulnificus		
YJ016	Clinical isolate	(Shao and Hor, 2000)
VVA0326^{-}	VVA0326 mutant in YJ016	This study
VVA0328^{-}	VVA0328 mutant in YJ016	This study
RtxL^{-}	VVA0331 mutant in YJ016	This study
VVA0326^{-}VVA0328^{-}	VVA0326 and VVA0328 double mutant in YJ016	This study

Table 2. Bacterial plasmids used and constructed in this study

Plasmids	Relevant characteristic	Source or reference
pGEM-Teasy	PCR cloning vector, Ap^r	Promega
yT&A vector	PCR cloning vector, Ap^r	Yeastern Biotech
TOPO TA vector	PCR cloning vector, Ap^r	Invitrogen
pET-30a-c	Expression vector, Km^r	Novagen
pCVD442	Suicide vector, Ap^r	(Donnenberg and Kaper, 1991)
pGFPuv	GFP expression vector, Ap^r	Laboratory collection
Constructs related to *VVA0326*⁻ mutant		
pVV_3	1 kb fragment amplified using primer pairs, VV-3L and VV-3R, and cloned into pGEM-T vector, Ap^r	This study
pVV_4	1 kb fragment amplified using primer pairs, VV-4L and VV-4R, and cloned into yT&A vector, Ap^r	This study
pVV_3-4	*Bam*HI/*Xba*I-digested fragment of pVV_4 subcloned into pVV_3, Ap^r	This study
p3-4_Gm	*Sac*I/*Xba*I-digested fragment of pVV_3-4 subcloned into pCVD442, Ap^r	This study
Constructs related to *VVA0328* mutant		
pVV_7	1 kb fragment amplified using primer pairs, VV-7L and VV-7R, and cloned into yT&A vector, Ap^r	This study
pVV_8	1 kb fragment amplified using primer pairs, VV-8L and VV-8R, and cloned into yT&A vector, Ap^r	This study
pVV_7-8	*Bam*HI-igested fragment of pVV_8 subcloned into pVV_7, Ap^r	This study
p7-8_Em	*Sac*I/*Xba*I-digested fragment of pVV_7-8 cubcloned into pCVD442, Ap^r	This study
Constructs related to *VVA0331* mutant		
pVV_9	1 kb fragment amplified using primer pairs, VV-9L and VV-9R, and cloned into yT&A vector, Ap^r	This study
pVV_10	1 kb fragment amplified using primer pairs, VV-10L and VV-10R, and cloned into yT&A vector, Ap^r	This study
pVV_9-10	*Bam*HI-digested fragment of pVV_10 subcloned into pVV_9, Ap^r	This study
p9-10_RTXm	*Sma*I/*Xba*I-digested fragment of pVV_9-10 cubcloned into pCVD442, Ap^r	This study
Constructs related to GFP fusion protein		
pGGDEF	GGDEF coding region amplified using primer pairs, Gp1 and Gp2, and cloned into TOPO TA vector, Ap^r	This study
pEAL	EAL coding region amplified using primer pairs, Ep1 and Ep2, and cloned into TOPO TA vector, Ap^r	This study
pVVA0326-GFP	*Hin*dIII/*Kpn*I-digested fragment of pGGDEF subcloned into pGFPuv, Ap^r	This study
pVVA0328-GFP	*Hin*dIII/*Kpn*I-digested fragment of pEAL subcloned into pGFPuv, Ap^r	This study

Table 3. Primers used in this study

Primer name	Oligo sequence
VV-1-L	5'-GGTAGGCGTTCGTGTGGA-3'
VV-1-R	5'-CAGTCGAGGATCCGCTTAGT-3'
VV-2-L	5'-TCCATGGATCCTAAGTTCTGTTT-3'
VV-2-R	5'-TCCACCATCTAGAACGACAGC-3'
VV-3-L	5'-CCCAGATGGAAATGTATAGCAC-3'
VV-3-R	5'-AGAATTGAGGATCCAAGCAGA-3'
VV-4-L	5'-ATTGTGGATCCCGGTTAGC-3'
VV-4-R	5'-CGCACACCGTCTAGAAAGTATT-3'
VV-5-L	5'-GCTCGTCTTTGATCACCTCG-3'
VV-5-R	5'-AATTTTGTGGATCCGCGA-3'
VV-6-L	5'-TGGGATCCGATGCGTCTT-3'
VV-6-R	5'-GATCAGTGCTCTAGACCGCC-3'
VV-7-L	5'-CGGCATAAATAGCCAGTGC-3'
VV-7-R	5'-TCAGGTGGATCCAAGCGTT-3'
VV-8-L	5'-CAGTGGGATCCACAAGTCAAT-3'
VV-8-R	5'-AACGCCACATCTAGAATATCCC-3'
VV-8-L2	5'-CCGGATCCAGTTCAGAGATC-3'
VV-8-R2	5'-CTCTAGAAGCAAATGGGTGGTC-3'
VV-9-L	5'-CGGTAAGCATTGACTCTGGC-3'
VV-9-R	5'-CGTACCTTGGATCCTCAGCTC-3'
VV-10-L	5'-GTGACGGATCCCTCTGGTG-3'
VV-10-R	5'-CGTGCCAGGTACTTCTAGAGC-3'
VV-11-L	5'-CGTAATGCTCGTGGATGCT-3'
VV-11-R	5'-AATTGCACTCGGATCCGC-3'
VV-12-L	5'-ATAACGGATCCAGCCAACAT-3'
VV-12-R	5'-TGAAACTCTAGACGCCGGTG-3'
LPRepeat1	5'-TTCCTCCCATGGTTGACAGCGCG-3'
LPRepeat2	6'-CGAAGCGGCCGCGGTAATGGTGA-3'
LPCys1	7'-GCTGATCCCCATGGATGCGACG-3'
LPCys2	8'-GCGGCCGCTCACTGGTTGGCTTG-3'
Gp1	5'-AAGCTTCAATCACCACCATCAGCCG-3'
Gp2	5'-GGTACCCGGCGGCTCTCCTTGACT-3'
Ep1	5'-AAGCTTATCTCTGAACTGGATGCGG-3'
Ep2	5'-GGTACCGCGCTCAATATATTGATTGC-3'

Table 4. Annotation of the gene clusters contained in the genomic island.

Genes	Predicted function
VVA0325	Putative two-component response regulator
VVA0326	GGDEF family protein
VVA0327	Putative two-component Response regulator
VVA0328	Response regulator VieA containing EAL domain
VVA0329	Probable sensor kinase VieS
VVA0330	Conserved hypothetical protein
VVA0331	Rtx-like protein
VVA0332	Toxin secretion ATP-binding protein, HlyB like
VVA0333	Secretion protein, HlyD like
VVA0334	Agglutination protein, TolC like

Table 5. Amino acid sequence identity and similarity of the VieSA gene clusters.

	Similarity / Identity	VvVieS2 (VVA0647)	VvVieS1 (VVA0329)	VcVieS (VC1651)	VpVieS (VPA7036)
Chromosome II	VvVieS2 (VVA0647)		52%	66%	50%
Chromosome II	VvVieS1 (VVA0329)	32%		50%	64%
Chromosome I	VcVieS (VC1651)	50%	30%		49%
Chromosome II	VpVieS (VPA7036)	30%	44%	29%	

	Similarity / Identity	VvVieA2(589) (VVA0648)	VvVieA1(387) (VVA0328)	VcVieA(585) (VC1650)	VpVieS(390) (VPA7037)
Chromosome II	VvVieA2(589) (VVA0648)		54%	70%	54%
Chromosome II	VvVieA1(387) (VVA0328)	34%		56%	71%
Chromosome I	VcVieA(585) (VC1650)	54%	36%		54%
Chromosome II	VpVieS(390) (VPA7037)	33%	55%	33%	

Table 6. Inventory of GGDEF- and EAL- proteins in the selected bacterial genomes.

Spicies	Genome size (kb)	GGDEF	EAL	GGDEF_EAL	(a)Cellulose synthesis genes	(b)Flagellar synthesis genes
Aquifex aeolicus VF5	1.59	11	7	4	+	+
Thermotoga maritima MSB8	1.86	9	0	0	-	+
Haemophilus influenzae Rd KW20	1.83	0	0	0	-	-
Shewanella oneidensis MR-1	5.13	52	29	20	-	+
Pseudomonas aeruginosa PAO1	6.26	33	21	16	-	+
Pseudomonas putida KT2440	6.18	36	21	17	+	+
Pseudomonas syringae pv. tomato str. DC3000	6.54	35	21	19	+	+
Shigella flexneri 2a str. 2457T	4.6	8	7	2	+	+
Yersinia pestis KIM	4.6	7	6	3	-	+
Escherichia coli K12	4.64	23	16	7	+	+
Escherichia coli O157:H7	5.5	19	15	6	+	+
Salmonella enterica subsp. enterica serovar Typhi Ty2	4.79	11	13	5	+	+
Salmonella typhimurium LT2	4.95	11	12	5	+	+
Vibrio cholerae O1 biovar eltor str. N16961	4.03	41	22	10	-	+
Vibrio parahaemolyticus RIMD 2210633	5.17	44	29	16	-	+
Vibrio vulnificus YJ016	5.26	65	32	18	-	+
Xanthomonas campestris pv. campestris str. ATCC 33913	5.08	30	14	8	+	+
Xylella fastidiosa 9a5c	2.73	2	3	1	-	-
Agrobacterium tumefaciens str. C58	5.67	29	15	12	+	+
Rickettsia conorii str. Malish 7	1.27	1	1	0	-	-
Campylobacter jejuni subsp. jejuni NCTC 11168	1.64	1	0	0	-	+
Helicobacter pylori J99	1.64	0	0	0	-	+
Bordetella pertussis Tohama I	4.09	7	3	2	-	+
Neisseria meningitidis MC58	2.27	0	0	0	-	-
Clostridium acetobutylicum ATCC 824	4.13	10	4	3	-	+
Listeria monocytogenes str. 4b F2365	2.99	3	3	0	-	+
Bacillus anthracis str. Ames	5.23	8	7	6	+	+
Bacillus cereus ATCC 14579	5.43	6	5	4	+	+
Staphylococcus aureus subsp. aureus MRSA252	2.9	1	0	0	-	-
Staphylococcus epidermidis ATCC 12228	2.5	1	0	0	-	-
Enterococcus faecalis V583	3.36	0	0	0	-	-
Lactococcus lactis subsp. lactis Il1403	2.37	0	0	0	-	-
Streptococcus agalactiae 2603V/R	2.16	0	0	0	-	-
Streptococcus mutans UA159	2.03	0	0	0	-	-
Streptococcus pneumoniae R6	2.04	0	0	0	-	-
Streptococcus pyogenes M1 GAS	1.85	0	0	0	-	-
Mycoplasma genitalium G-37	0.58	0	0	0	-	-
Mycoplasma pneumoniae M129	0.82	0	0	0	-	-
Streptomyces coelicolor A3(2)	9.05	9	5	4	-	-
Corynebacterium diphtheriae NCTC 13129	2.49	0	0	0	-	-
Mycobacterium leprae TN	3.27	3	2	1	-	-
Mycobacterium bovis AF2122/97	4.35	1	2	1	-	-
Mycobacterium tuberculosis H37Rv	4.41	1	2	1	-	-
Borrelia burgdorferi B31	1.52	1	1	0	-	+
Treponema pallidum subsp. pallidum str. Nichols	1.14	1	0	0	-	+
Chlamydia trachomatis D/UW-3/CX	1.04	0	0	0	-	-
Chlamydophila pneumoniae AR39	1.23	0	0	0	-	-
Deinococcus radiodurans R1	3.28	16	4	4	-	-

(a) A positive sign means the genome cotanins at least one of the cellulose synthesis genes

(b) A positive sign means the genome cotanins at least one of the flegallar synthesis genes

Figures

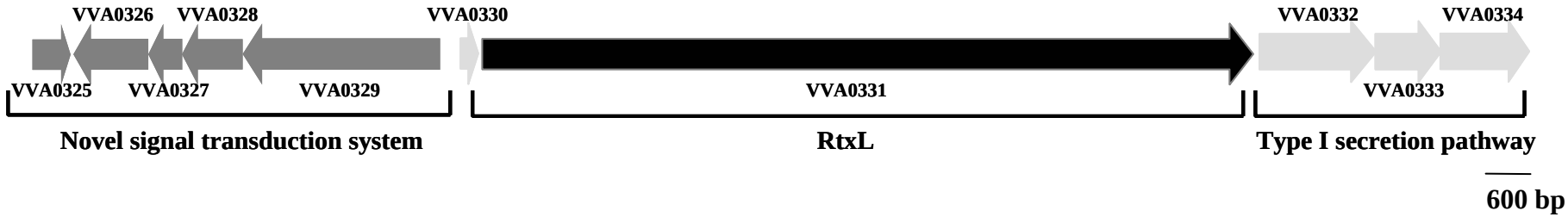

Fig. 1. Genetic structure of the virulence-associated island. The arrows indicate the lengths of the gene fragments and directions of the transcripts.

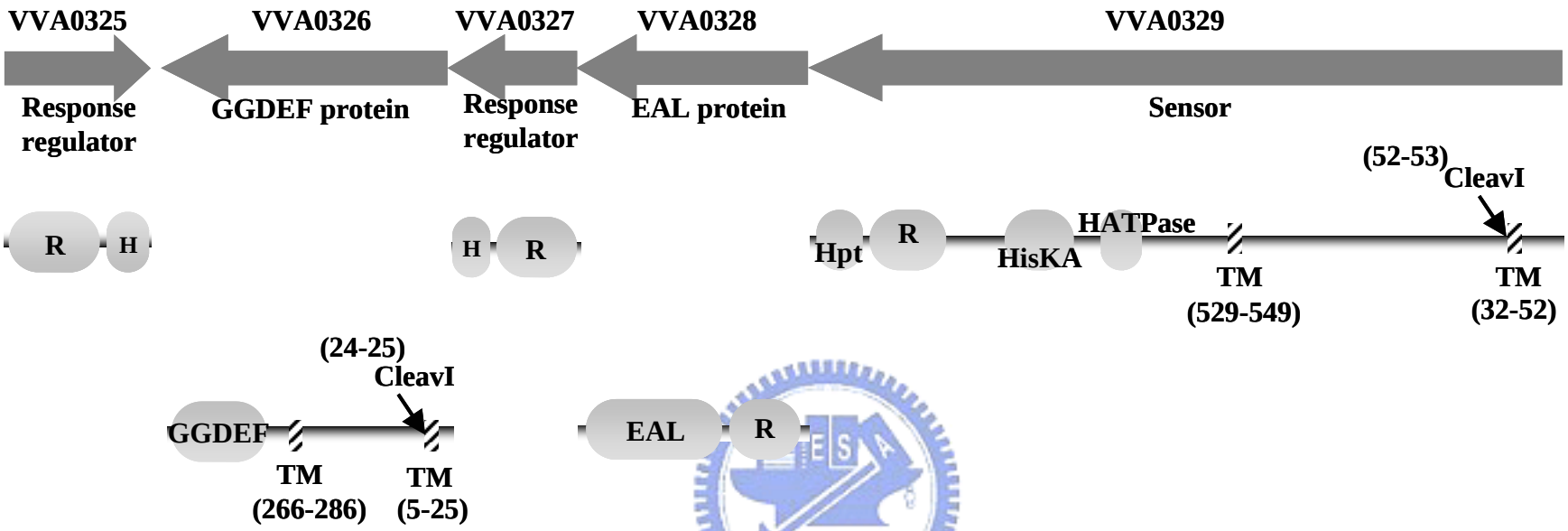

Fig. 2. Schematic diagram of the signal transduction system. The protein translated from each ORF is shown under the gene and the functional domains are labeled. R: Response regulator receiver domain; H: "Helix-turn-helix" DNA binding motif (luxR family); GGDEF: diguanylate cyclase domain; EAL: phosphodiesterase domain; HisKA: His Kinase A phosphoacceptor domain; HATPase: histidine kinase; Hpt: histidine-containing phosphotransfer domain; CleavI: cleavage site for signal peptidase I; TM: Transmembrane.

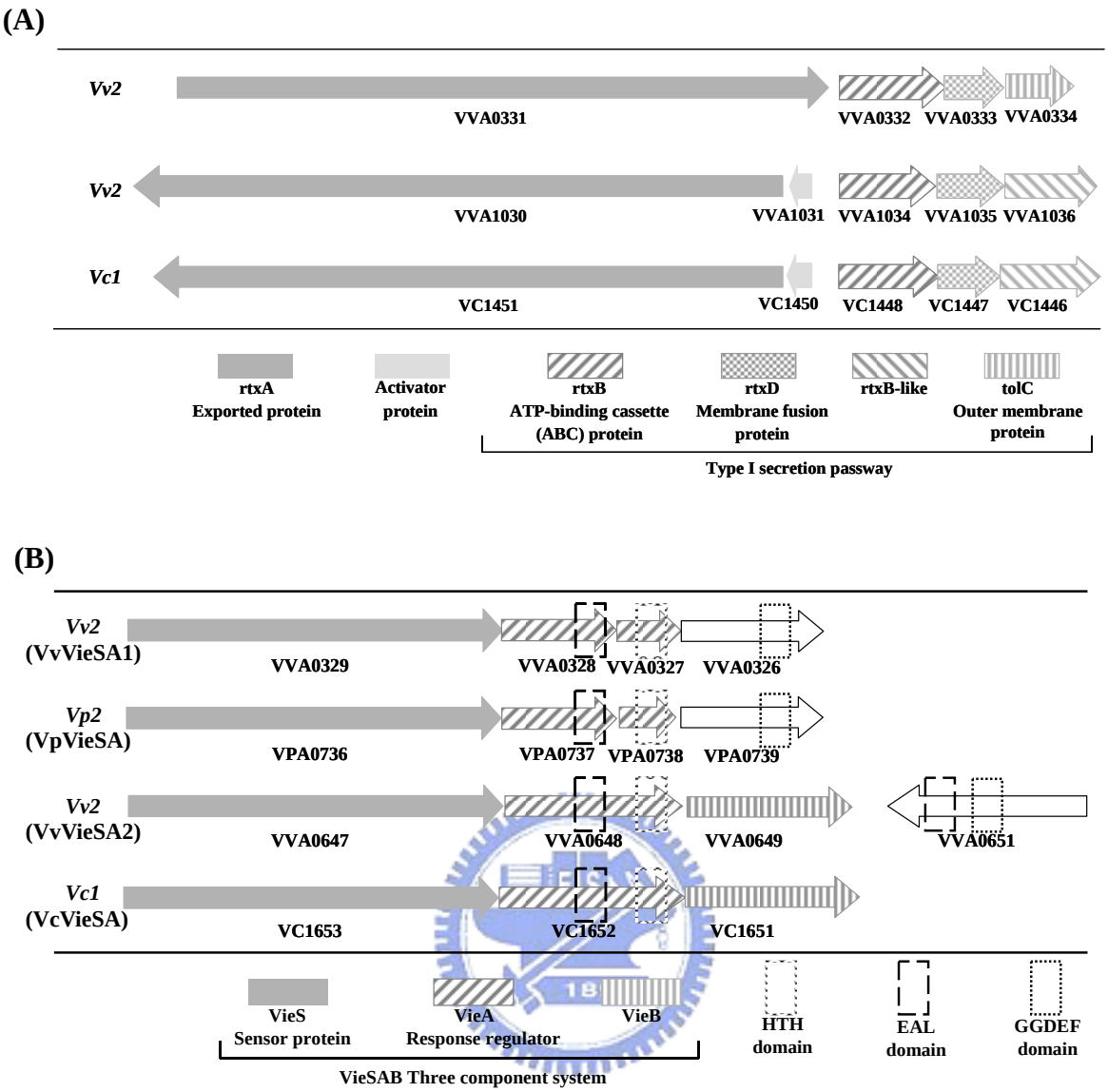

Fig. 3. Comparative analysis of rtxL (A) and vieSAB-like gene clusters (B). The diagrams (not to scale) depict the gene clusters and paralogous members in *V. vulnificus* YJ016 (*V.v*) and the corresponding genes in *V. cholerae* El Tor N16961 (*V.c*) and *Vibrio parahaemolyticus RIMD 2210633* (*V.p*). The numbers, 1 and 2 after the bacterial abbreviation represent the large and small chromosome respectively.

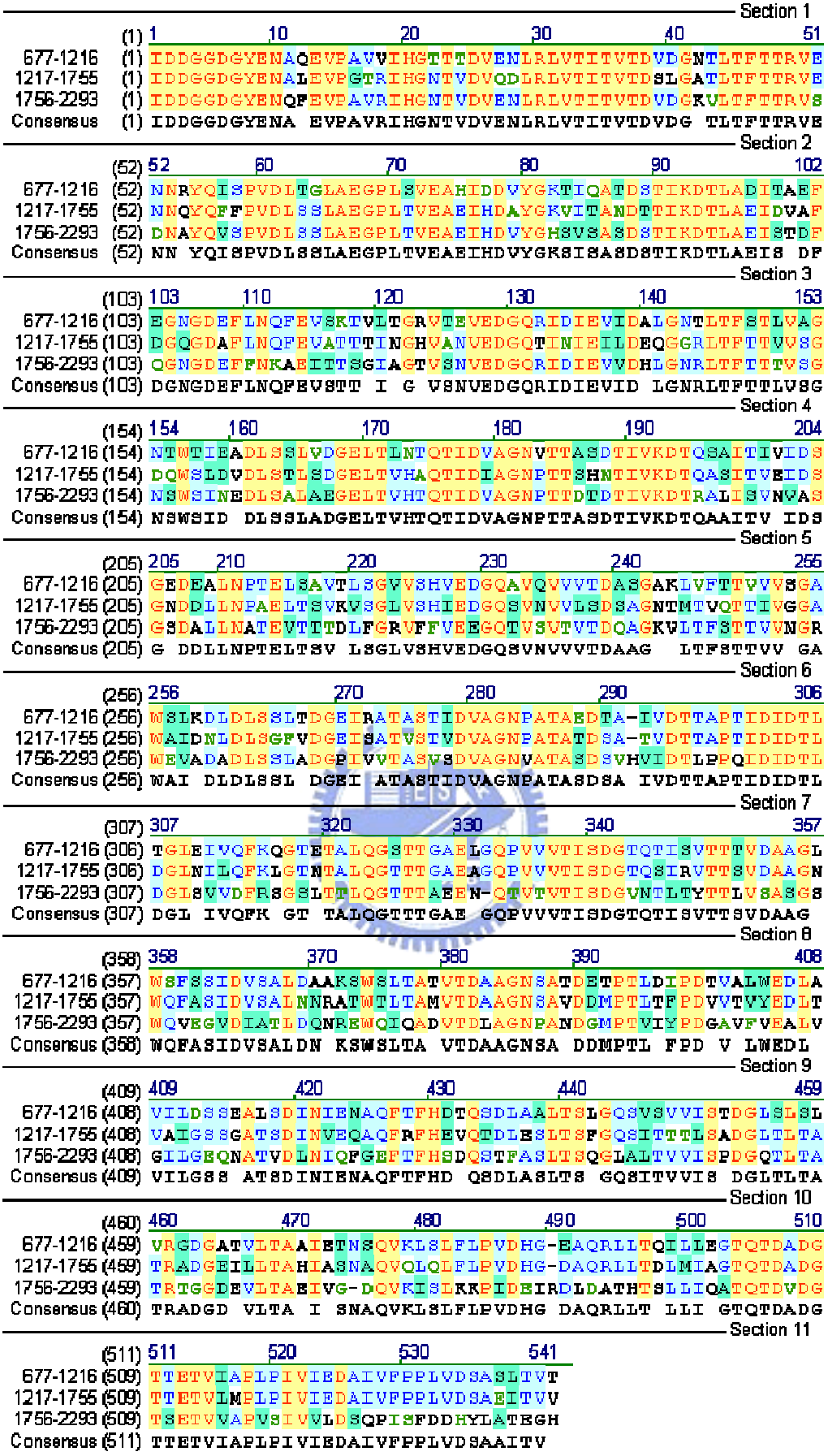

Fig. 4. Three repeats of 539 a.a in length of RtxL protein. The three repeats are respectively from 677 to 1216; 1217 to 1755, and 1756 to 2293.

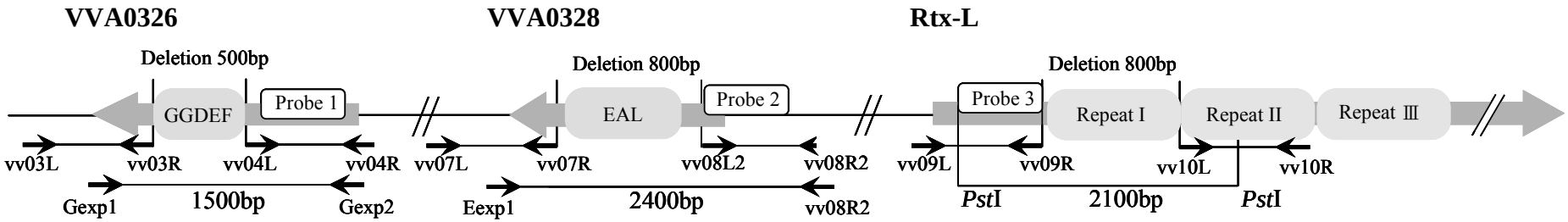

Fig. 5A. Construction of the deletion mutants. The deletion region for each is indicated. The primers used in the PCR-amplified DNA fragments are indicated as arrow bar and each of the probes used to analyze the mutants. In southern blotting hybridization is indicated as white frame. Grey frame represent the motifs of GGDEF and EAL and the repeat of RtxL.

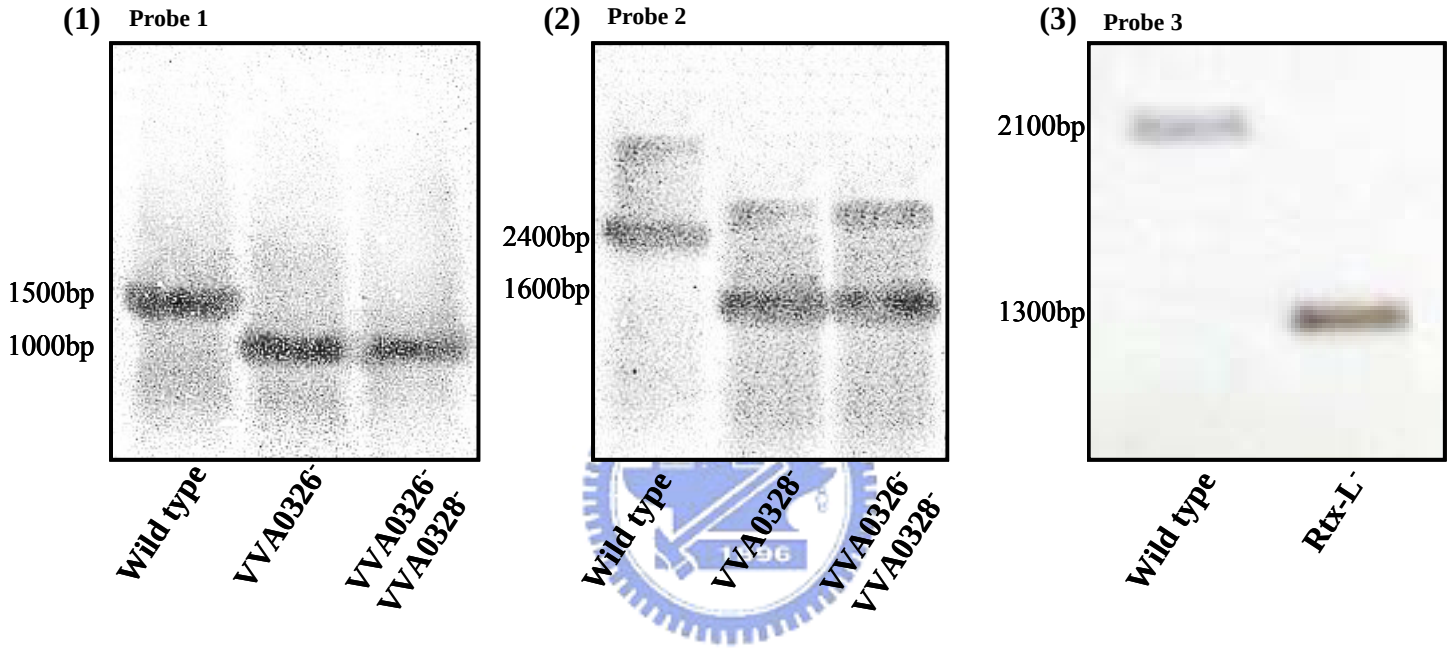

Fig. 5B. Southern blot analysis of the mutants. The hybridization using probe 1 to (1), probe 2 to (2), and probe 2 to (3) are shown. (1) The PCR products were amplified by the primer pair Gexp1and Gexp2. (2) PCR products were amplified by the primer pair Eexp1and vv08R2 (C) The chromosomal DNA digested with *Pst*I.

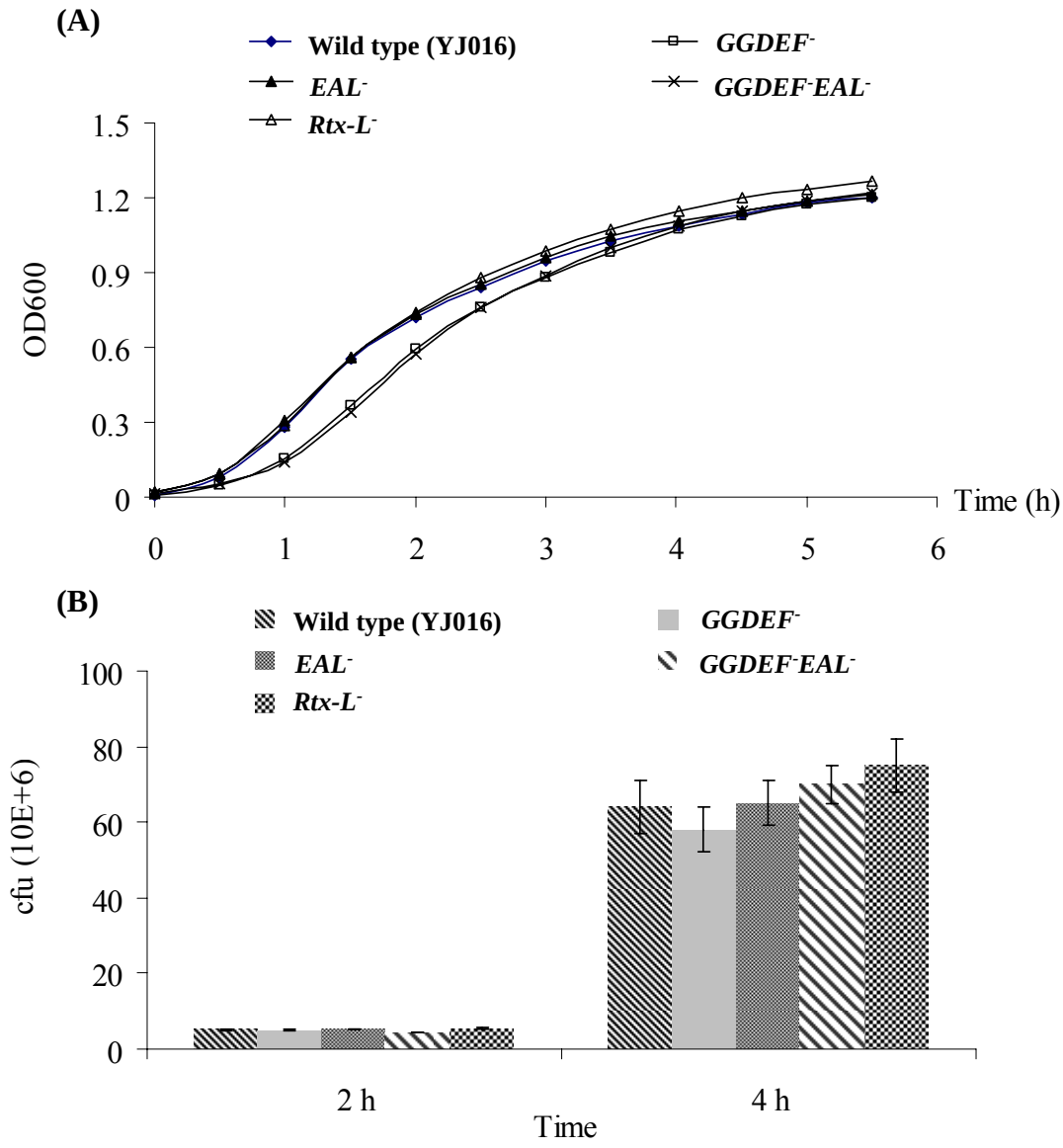

Fig. 6. Analysis of the growth of wild type and the derived mutants. (A)The growth curve was determined by measuring the optical density at 600 nm (OD_{600}). (B) The number of bacteria was measured when the broth in either 2 h or 4 h plated on LB agar plate for the colony forming units (CFU).

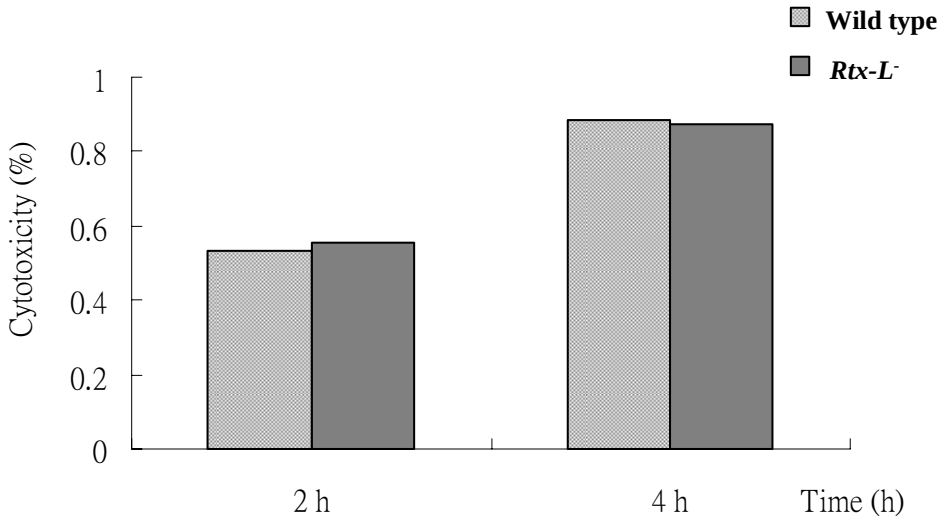

Fig. 7. Cytotoxicity analysis of wild type and RtxL mutants. After incubating at 37°C either 2 h or 4 h, the cytotoxicity was determined by measuring the activity of lactate dehydrogenase (LDH), a cytosolic enzyme released upon cell lyses, in the supernatant. LDH activity was assayed with a commercial kit (CytoTox 96 nonradioactive cytotoxicity assay; Promega) and was expressed as % Cytotoxicity = (Experimental – Effector Spontaneous – Target Spontaneous) / (Target Maximum – Target Spontaneous) ×100%

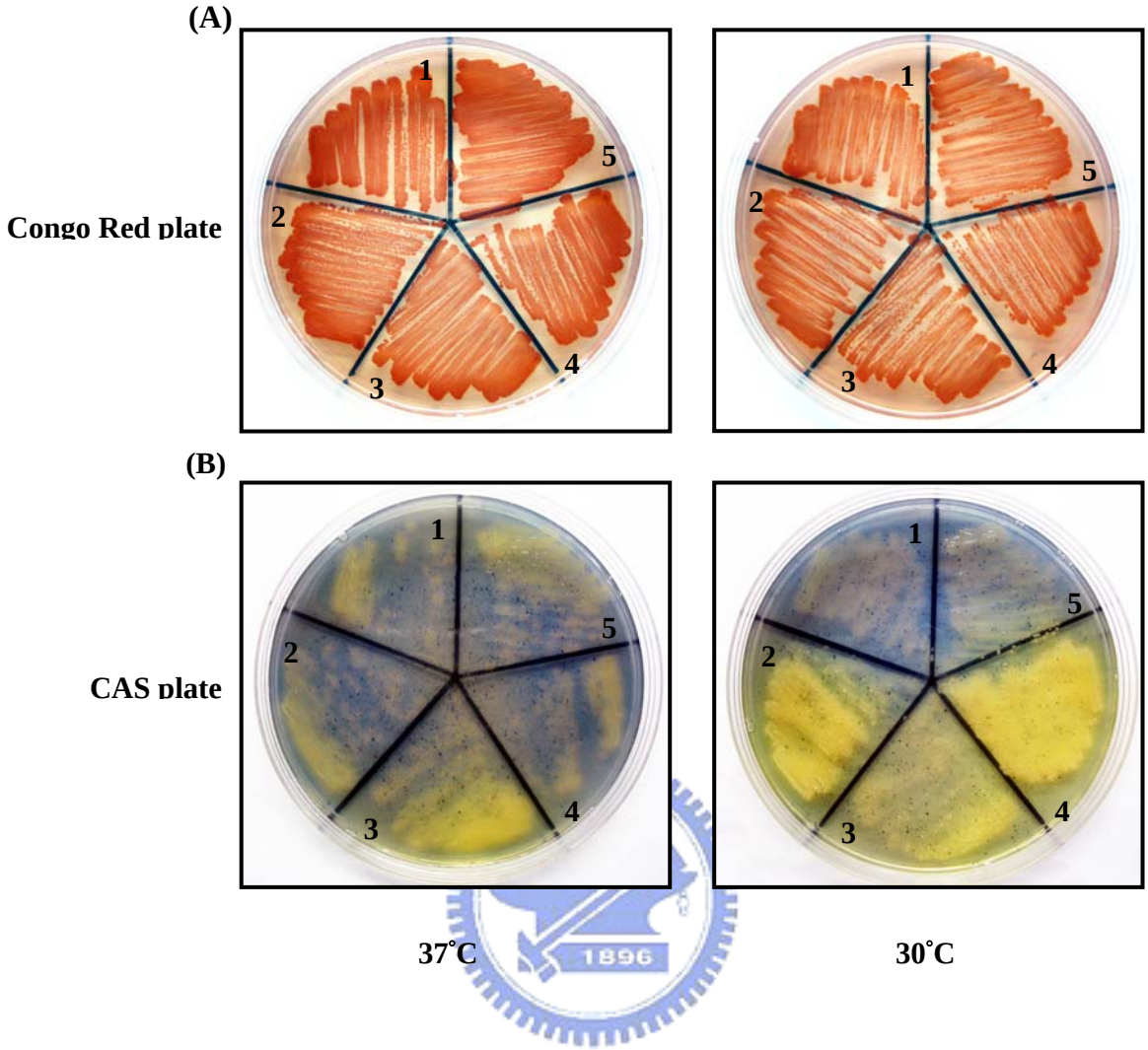

Fig. 8. Morphotypic analysis of wild type and the derived mutants by Congo-Red (A) and CAS (B) agar plate. The photographs were taken after the bacteria incubated for 24 h at 37 °C and 30 °C. 1: YJ016 (wild type); 2: VVA0326^{-}; 3: VVA0328^{-}; 4: VVA0326^{-}VVA0328^{-}; 5: *rtxL*$^{-}$. On the blue CAS medium, iron chelation results in a chemically induced color change to bright orange; thus, strains which produce siderophores are easily distinguished.

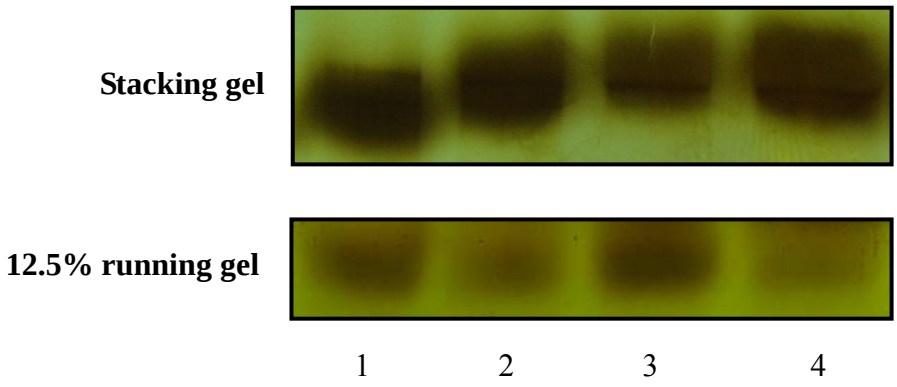

Fig. 9. SDS-PAGE analysis of polysaccharide extracted from the wild type and derived mutant strains. Gel was determined by silver stains. 1: YJ016 (wild type); 2: VVA0326$^-$; 3: VVA0328$^-$; 4: VVA0326$^-$VVA0328$^-$.

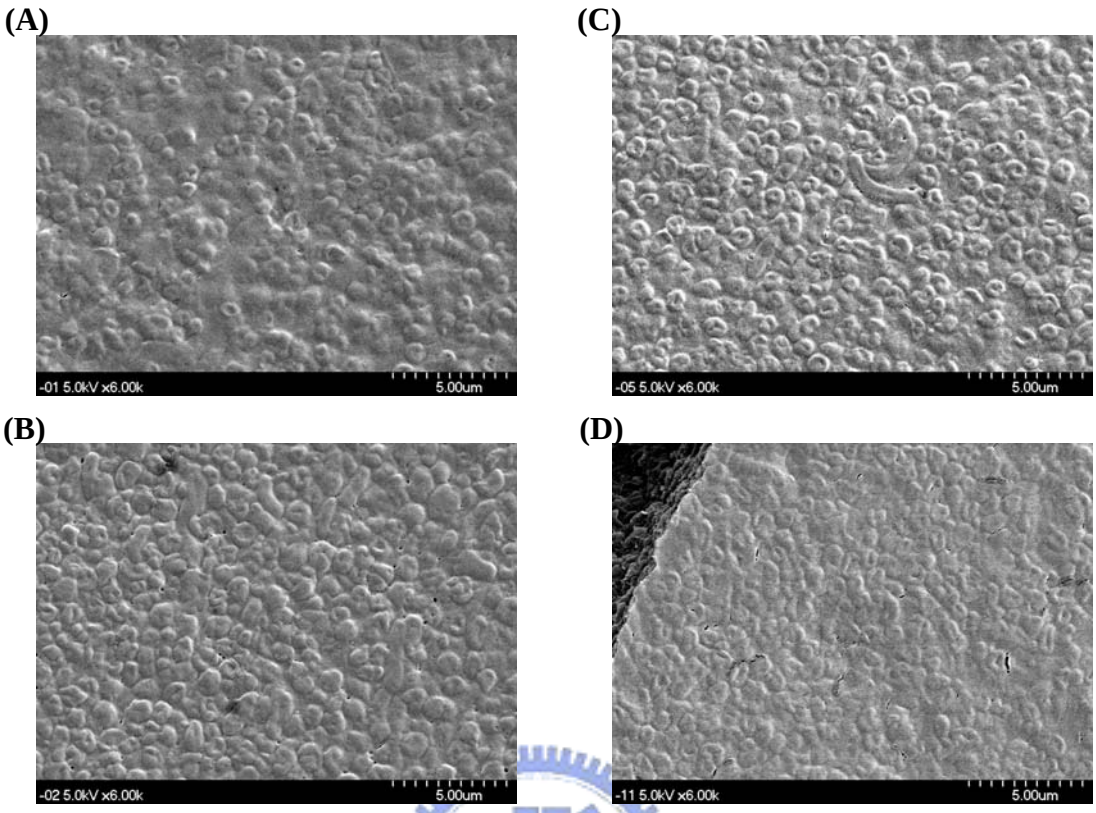

Fig. 10. Scanning electron microscopy of plate grown cells. (A) YJ016 (wild type); (B) VVA0326$^-$; (C) VVA0328$^-$; (D) VVA0326$^-$VVA0328$^-$. ×6,000.

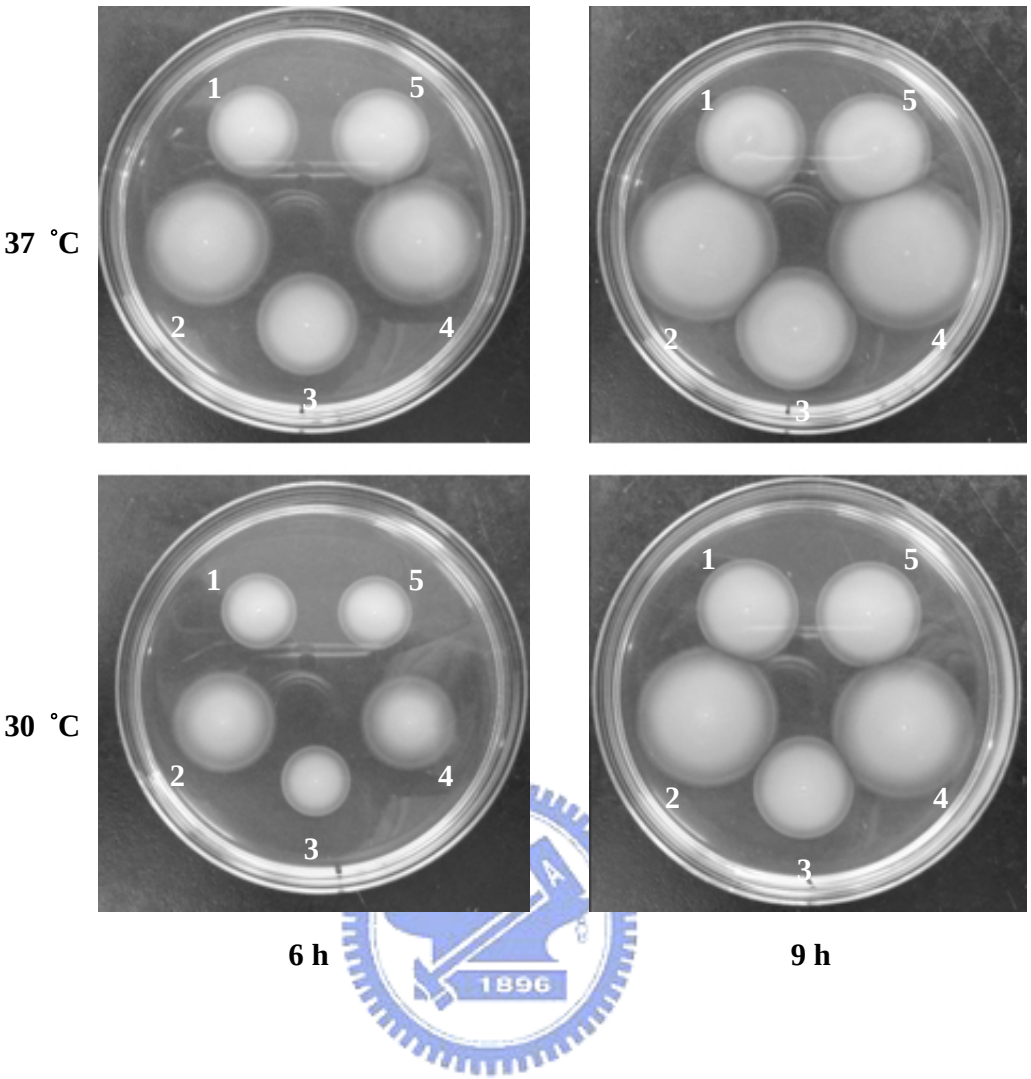

Fig. 11. Swimming assay of wild type and the derived mutants. The analyses were performed as described in materials and methods. The photographs were taken after the bacteria incubated for 6 h and 9 h at 37 °C and 30 °C. 1: YJ016 (wild type); 2: VVA0326^{-}; 3: VVA0328^{-}; 4: VVA0326^{-}VVA0328^{-}; 5: *rtxL*$^{-}$.

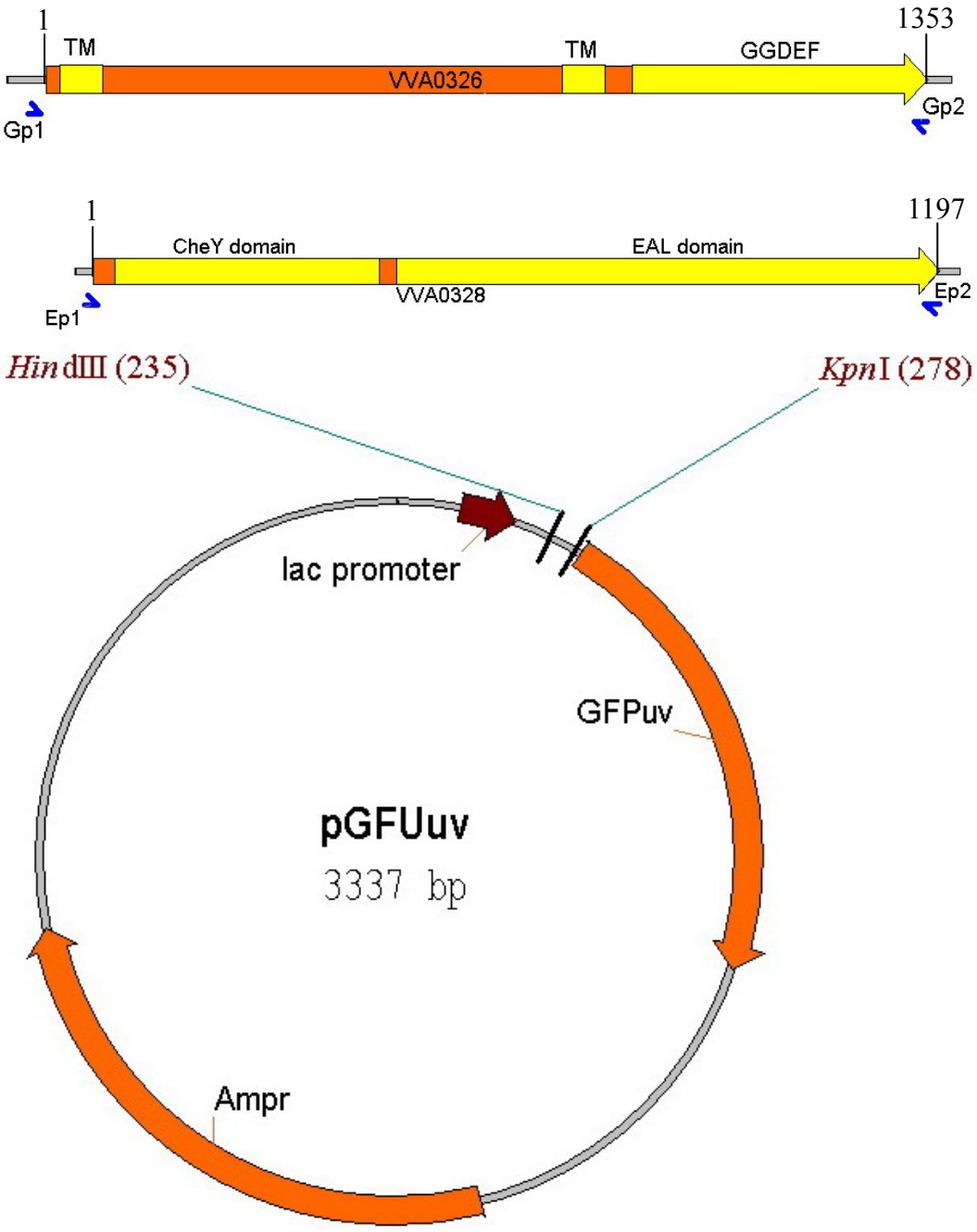

Fig. 12A. Physical map of pVVA0326-GFP and pVVA0328-GFP. The primer pairs Gp1/Gp2 and Ep1/Ep2 were used respectively to amplify the coding regions of VVA0326 and VVA0328, and also introduce adjacent *Hin*dIII and *Kpn*I restriction sites. The *Hin*dIII-*Kpn*I fragments of VVA0326 and VVA0328 were then subcloned in frame fusion to *gfp* gene of pGFPuv.

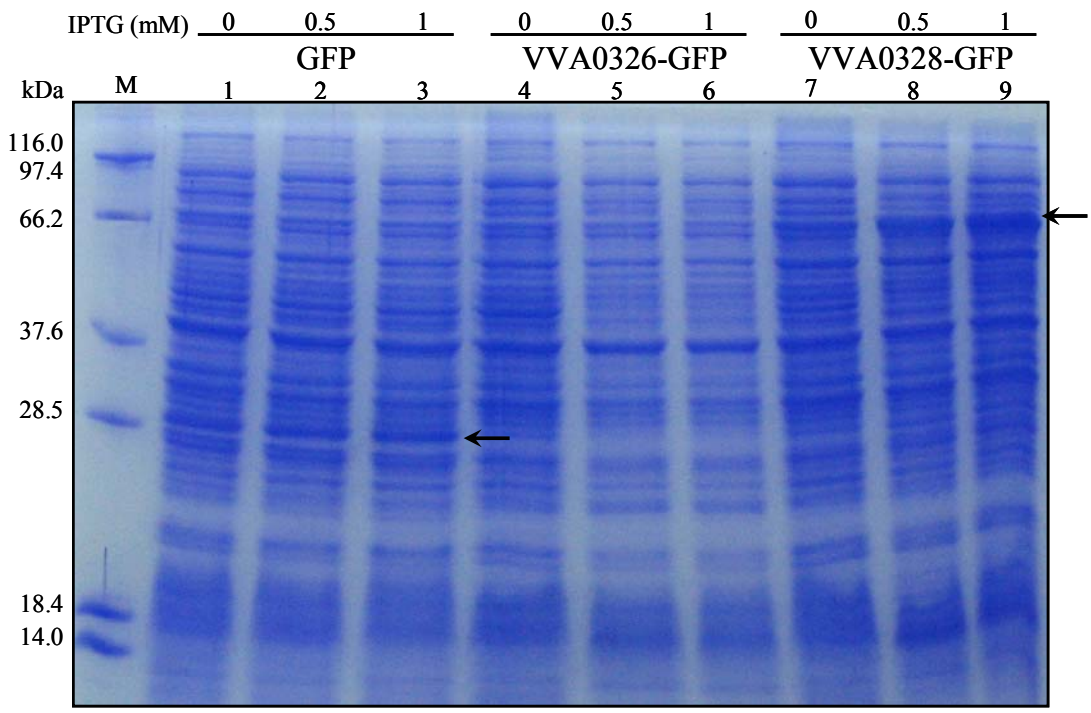

Fig. 12B. SDS-PAGE analysis of the GFP, VVA0326-GFP and VVA0328-GFP recombinant protein expressed in E. coli JM109. The arrows indicate the predicted recombinant proteins. The sample in each lane was prepared from the cells carrying the each of the following plasmids: Lanes 1-3: pGFP; Lanes 4-6: pVVA0326-GFP; Lanes 7-9: pVVA0328-GFP. The bacteria were cultured and harvested 4 h after the bacteria induced with IPTG (0.5 or 1 mM). M: protein markers. Lanes 1, 4, 7: noniduced total cell lysate; Lanes 2, 5, 8: the total cell lysates induced with 0.5 mM IPTG; Lanes 3, 6, 9: the total cell lysates induced with 1 mM IPTG.

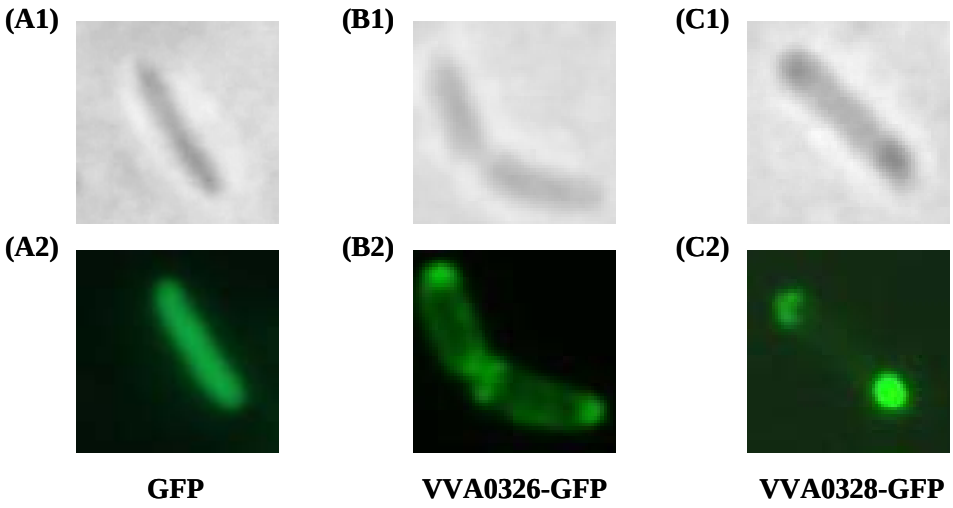

Fig. 13. Localization of the recombinant proteins VVA0326-GFP and VVA0328-GFP in E. coli JM109. (A) GFP (pGFP); (B) VVA0326-GFP (pVVA0326-GFP); (C) VVA0328-GFP (pVVA0328-GFP). The panels were photographed with an epifluorescence microscope; A1 to C1 were taken with a normal light source and A2 to C2 were taken with an excitation light.

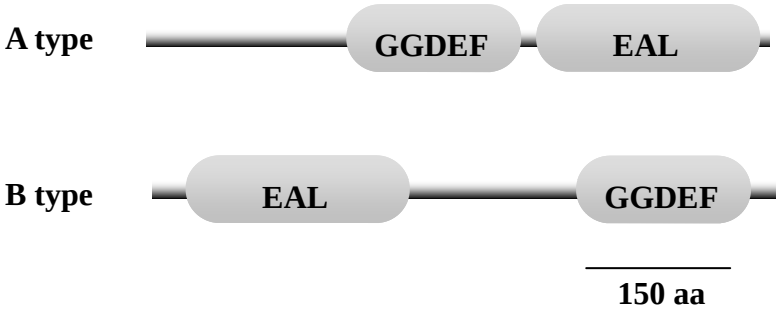

Fig. 14. Domain organization of the sequenced both GGDEF- and EAL-containing proteins.

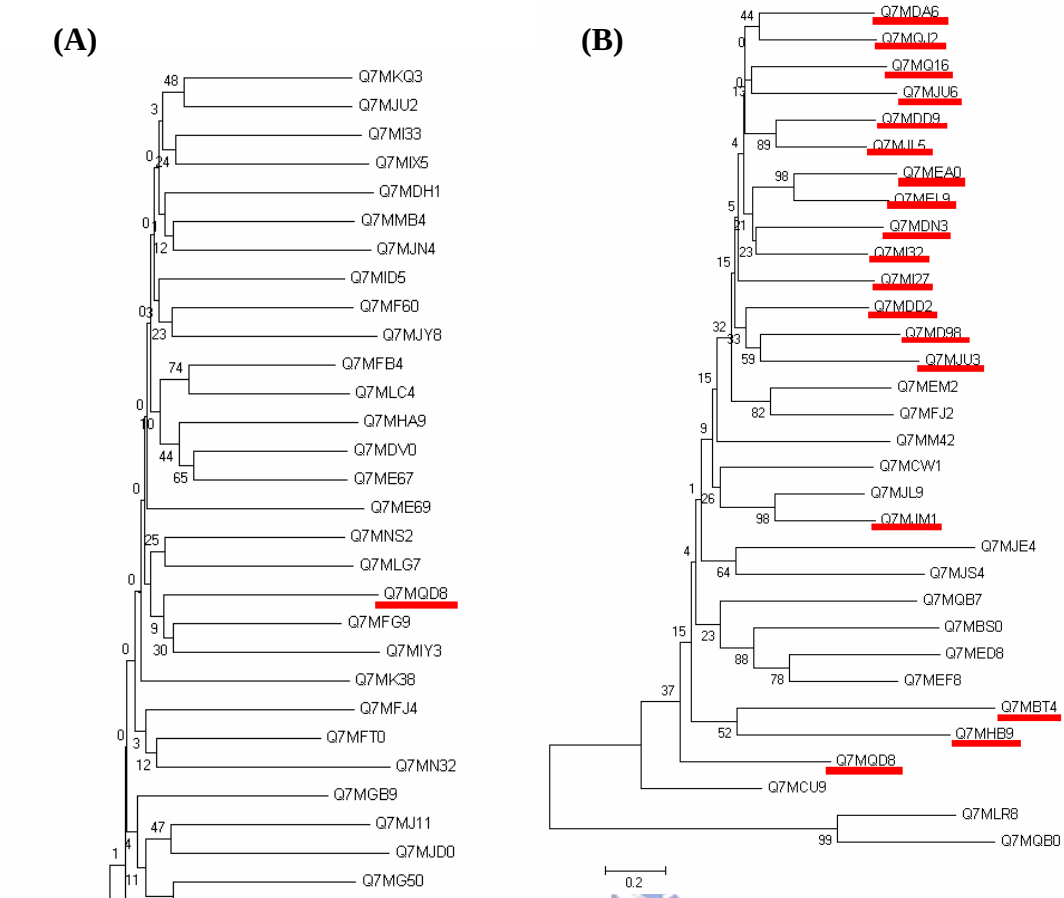

Fig. 15. Phylogenetic trees of the 63 GGDEF-containing (A) and 31 EAL-containing (B) proteins in *V. v* YJ016. The trees were constructed by CLUSTALW using the deduced amino acid sequences and performed by MEGA program. The bootstrap values generated by 1000 sets of replications of tree construction are labeled at the internal nodes of the un-rooted trees. The GGDEF-EAL proteins are underlined.

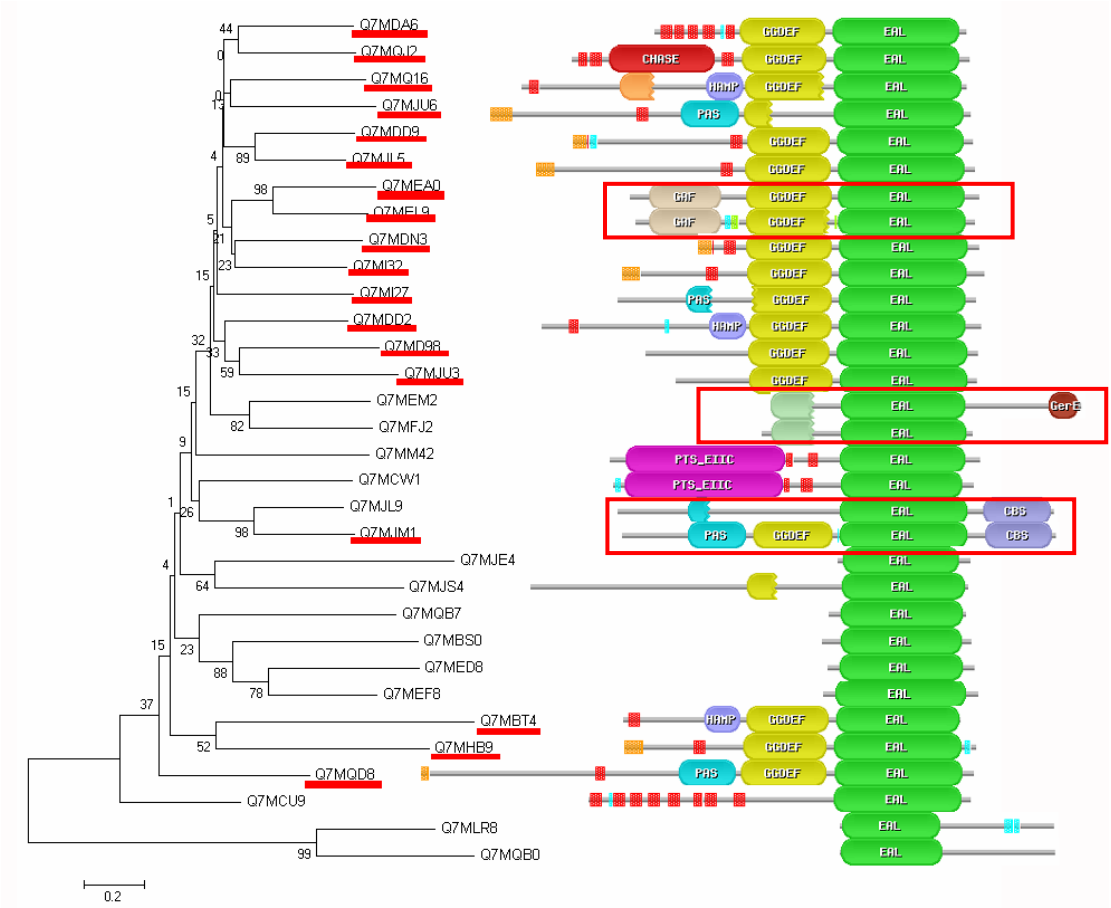

Fig. 16. Comparing phylogenetic trees with the domain structure of the EAL-containing proteins. The framed parts indicated the likely duplicated proteins.

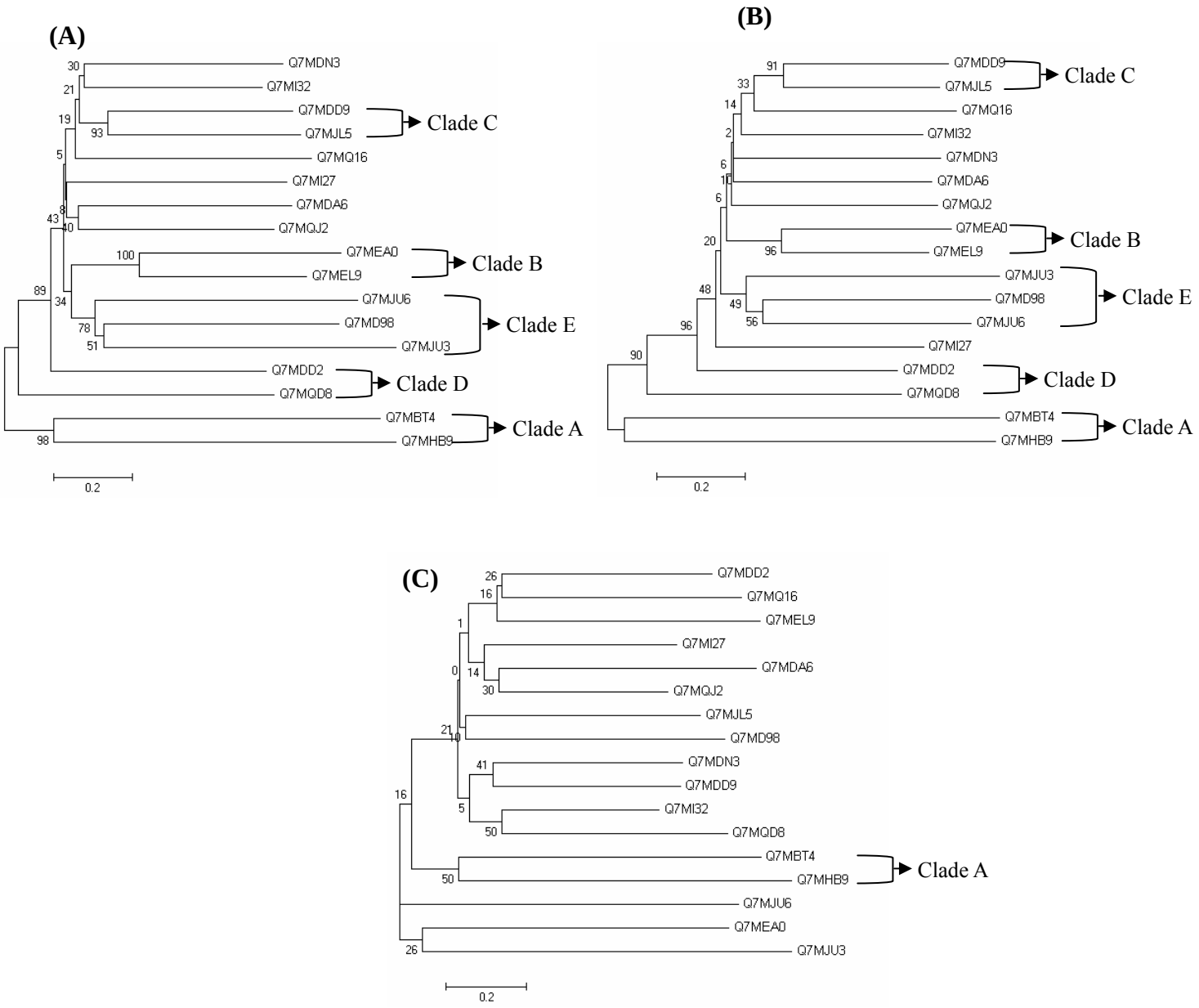

Fig. 17. Phylogenetic trees of the 18 GGDEF-EAL proteins. The 18 proteins containing both GGDEF and EAL domain from *V. vulnificus* YJ016 were defined according to the Pfam database. The tree topologies depicted represent (A) GGDEF and EAL domain; (B) EAL domain; (C) GGDEF domain. The congruent clades respectively in the trees are labeled from A to E.